Thermochimica Acta, 5 (1972) 173–220

PURITY DETERMINATION BY DIFFERENTIAL SCANNING CALORIMETRY

ERWIN E. MARTI

Central Research Services Department, Ciba–Geigy Ltd., Basel (Switzerland)

(Received April 3rd, 1972; revised June 23rd, 1972)

ABSTRACT

A review of the literature on the DSC method for purity determination is presented, with a discussion of the most important aspects, *i.e.* theory, sample handling, calibration of the instrument, evaluation of melting curves, and the conditions and accuracy of the measurement of eutectic impurities.

A number of mathematical descriptions of the solid–liquid equilibrium for eutectic binary systems is applied to the calculation of theoretical phase diagrams and specific heat functions, which are then compared with experimental phase diagrams and melting curves. The applicability of the DSC method to systems of solid solutions is discussed.

Both the experimental procedure and the evaluation by computer methods required to obtain accurate impurity determinations by DSC are presented. A number of practical examples is included.

INTRODUCTION

The measurement of the melting point of a substance as a method of identification dates back to the early days of chemistry. Many different observations on organic and inorganic substances were made during the thermal treatment necessary for a melting point determination.

The observations were summarized and interpreted in terms of phenomena like polymorphism, sublimation, thermal decomposition, solid solutions, eutectic systems, congruently-melting compounds, glass transitions and others. Kofler[1] turned the melting point determination by microscopic observation into an extremely useful method in the field of analytical chemistry. Kofler's treatise on purity determinations is excellent, but of course, today, it is not easy to agree with the statement in *Thermomikromethoden*: "The method of purity determination with the microscopical observation of the melting point, however, will finally replace all the others". Somehow, the development of the analytical methods for purity determination since 1950 has appeared to prove the opposite, namely that all the other analytical methods would replace the melting point determinations. Kofler's melting point method is nowadays performed with many different types of apparatus. The method is used

because it is the simplest analytical method for getting information about the purity and about the crystal form of the sample under investigation. The melting point method is based on the determination of the absolute temperature of the substance assuming an infinitely small amount of solid substance in the solid–liquid equilibrium. A reference standard of a high purity is required to make the temperature measurement only a relative one. This high purity standard is also used for the relation between the purity and the melting point difference given in Eqn. (1)

$$\Delta T = T_1 - T_s = x_0 \cdot k_r \tag{1}$$

where ΔT is the melting point difference in °K, T_1 is the melting point of the high purity standard in °K, T_s is the melting point of the sample in °K, x_0 is the mole fraction of the impurity, and k_r is the cryoscopic constant in °K.

The cryoscopic constant is defined as

$$k_r = \frac{RT_1^2}{\Delta H_{f,1}} \tag{2}$$

where R is the gas constant and $\Delta H_{f,1}$ is the molar heat of fusion of the high purity standard, and is experimentally determined by means of Eqn. (1) or with a measurement of the heat of fusion $\Delta H_{f,1}$ and the melting point of the reference standard.

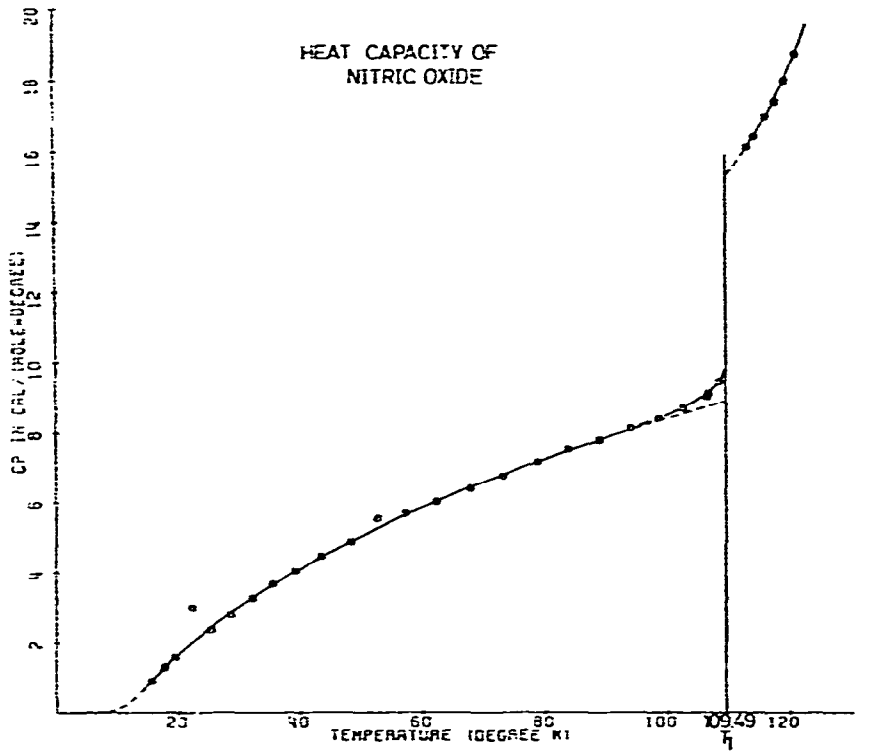

Fig. 1. Heat capacity of nitric oxide measured by Johnston and Giauque[3]. (Melting point T_1 = 109.49°K.)

Today, a second method seems to replace at least partially the microscopic observation of the melting point. This second method is known as differential scanning calorimetry (DSC). The DSC method measures the endothermic amount of energy which is afforded by the premelting process of substances. The method of premelting as a purity determination dates back to the 1920's in a form used by Eucken and Karwat[2] and Johnston and Giauque[3] for the measurement of the heat capacity of nitric oxide in the melting point region. In 1929, Johnston and Giauque[3] reported from the Chemical Laboratory of the University of California in Berkeley on the heat capacity of nitric oxide from 14°K to the boiling point.

The paper of Johnston and Giauque is interesting enough for a brief discussion. In Fig. 1, the heat capacity of nitric oxide is shown as a function of temperature, according to the measurements of Johnston and Giauque. The extremely sharp melting region of the nitric oxide sample at about 110°K should be noted. The nitric oxide used by Johnston and Giauque was produced by the reaction of potassium nitrite and potassium iodide in distilled water. The generated nitric oxide was purified over several distillation steps.

As an example, the same purified sample, containing $n_0 = 3.769$ moles of nitric oxide, was used for the premelting measurements and also the measurements of the heat capacity, the heat of fusion, and the melting point. Johnston and Giauque measured the following values for this sample of nitric oxide: molar heat of fusion, $\Delta H_{f,1} = 549.5 \pm 1.0$ cal.mole^{-1}; melting point, $T_1 \cong T_s = 109.49 \pm 0.05$°K.

The purity of the nitric oxide was calculated by applying Eqn. (3), which holds for low concentration of impurities

$$x_{0,2} = \frac{\Delta H_{f,1}}{RT_1^2}(T_1 - T)r \tag{3}$$

where $x_{0,2}$ is the eutectic impurity of the sample as mole fraction, $\Delta H_{f,1}$ is the molar heat of fusion of the pure nitric oxide, T_1 is the melting point of the pure nitric oxide, T is the temperature of the solid–liquid equilibrium, r is the molten fraction of the system at temperature T, and R is the gas constant.

The heat of premelting Δq_p, necessary for a temperature rise of the solid–liquid equilibrium from T' to T'', is related to the corresponding molten fractions of the sample r' and r''. We can write the equation

$$\Delta q_p = \Delta H_{f,1} n_0 (r'' - r') \tag{4}$$

The method of Johnston and Giauque enables the measurement of the total amount of heat Δq for a temperature rise of the substance from T' to T''. This total amount of heat is the sum of the heat of premelting Δq_p and an amount Δq_c given by the specific heat of the substance and the known temperature interval $\Delta T = T'' - T'$

$$\Delta q = \Delta q_p + \Delta q_c \tag{5}$$

The calculation of the heat of premelting (Δq_p) is possible from Eqn. (5), with the

measurement of the heat capacity of nitric oxide (Δq) and with an extrapolation of the specific heat from a region with practically no premelting into the selected region of premelting. The eutectic impurity of the nitric oxide is calculated for a corresponding set of temperatures and molten fractions (T', r'; T'', r'') and with the aid of Eqns. (3) and (4).

$$x_{0,2} = \frac{\Delta q_p}{n_0 R T_i^2} \cdot \frac{(T_i - T'')(T_i - T')}{T'' - T'} \tag{6}$$

With Eqn. (6) and the values of the measurements on nitric oxide, it is possible to calculate exactly the same values of eutectic impurities as found by Johnston and Giauque. The values and results are presented in Table I.

TABLE I
PREMELTING MEASUREMENTS ON NITRIC OXIDE

Temperatures (°K)		*Heat of premelting between T' and T'', q_p (cal)*	*Eutectic impurities $x_{0,2}$ (mole fraction)*
T'	T''		
104.71	108.59	0.171	7.9×10^{-6}
107.63	109.15	0.365	6.4×10^{-6}

Johnston and Giauque came to the conclusion that the nitric oxide used in their measurements contained less than 10^{-3} mole percent of eutectic impurities, or, the so-called purity is of the order of 99.999%. The authors excluded the possibility of noneutectic impurities because of the method of preparation of the nitric oxide used for these investigations. Johnston and Giauque explained that no analyses of the purified gas were made since accurate melting point and heat capacity data provide a more sensitive test of impurity than that given by chemical analysis. Johnston and Giauque made an equivalent statement to Kofler's about the measurement of impurities by the melting point method. It seems to be clear that such excellent investigators as Giauque and Kofler did not emphasize the melting point and premelting method in such a way without being deeply impressed by the possibilities of these two methods.

If we want to compare the excellent work from the low temperature laboratory at the University of California in Berkeley (the laboratory was named Giauque Hall in 1967) with the premelting measurements, mainly DSC and DTA, performed in the 1970's, we have to consider several points. The difference between the calorimetric method of Johnston and Giauque and the DSC or DTA method is not in thermodynamics but rather in the instrumentation and in the properties of the methods of measurement.

In Table II we compare some of the aspects of the two methods, selecting the DSC-IB of the Perkin–Elmer Corporation for the second group.

TABLE II

COMPARISON OF THE PREMELTING METHOD OF JOHNSTON AND GIAUQUE AND THE PURITY DETERMINATION WITH THE DSC-1B

Condition or property measured	*Calorimetric method of Johnston and Giauque*[3]	*DSC-1B (Perkin–Elmer Corp.)*
Weight of the sample	100 g	3 mg
Accuracy of the absolute temperatures	$\pm 10^{-2}$ °K	$\pm 3 \times 10^{-1}$ °K
Accuracy of the relative temperatures	$\pm 2 \times 10^{-3}$ °K	$\pm 10^{-2}$ °K
Accuracy of the measured heat of fusion	$\pm 2 \times 10^{-1}$ %	±5%
Accuracy in the purity value for high-purity substances	$\pm 10^{-4}$ %	$\pm 5 \times 10^{-2}$ %
Time for a premelting measurement	2–4 days	20 min

The great disadvantage of the calorimetric method developed by Johnston and Giauque, especially in industrial use, is the extremely long running time required for one measurement which is of course due to the enormous sample weights and the necessity for an equilibrium between the liquid and solid phases of the sample at all temperature points[4]. It is also clear, however, that somehow one has to pay for such a high accuracy in purity measurements. Between the measurements on purity with thermoanalytical methods of the 1920's and the 1970's, a great number of papers were published on purity measurements by the freezing point method. We mention only one paper, which we regard as representative of all the papers on thermoanalytical purity measurements produced during this period: Determination of Purity by Measurement of Freezing Points, by Glasgow, Krouskop, Beadle, Axilrod and Rossini[5].

Following these preliminary and historical remarks, we will concentrate on purity work performed with the DSC-IB, an instrument of the Perkin–Elmer Corporation. The development of new DSC- and DTA-systems will certainly change the issue of the purity determination, *e.g.* enhance the accuracy of the measurement of eutectic impurities and solid solutions without increasing the running time for one measurement.

DISCUSSION ON THE DSC LITERATURE ON PURITY

In this discussion we shall not attempt a complete report of the DSC literature. We will arrange our discussion according to theoretical and experimental points of the DSC-purity method.

(*a*) *Theory of the purity measurements*

As far as we know, all DSC results on purity in the literature are calculated

according to the following equation

$$T = T_1 - \frac{x_{0,2} R T_1^2}{\Delta H_{f,1}} \cdot \frac{1}{r} \tag{7}$$

[for symbols see Eqn. (3)].

Eqn. (7) is derived under the following approximations and conditions: (*i*) The components form a eutectic phase diagram; (*ii*) the system is at constant pressure; (*iii*) the impurity or impurities form ideal solutions with the molten part of the main component; (*iv*) the impurity is restricted to low concentrations; and (*v*) the heat of fusion is independent of temperature.

A second equation discussed by Driscoll and coworkers[6] describes systems containing eutectic impurities and impurities forming solid solutions with the main component. The systems of solid solutions are characterized according to Driscoll by a partition coefficient, this being the ratio of the concentrations of the impurity between the solid and liquid phases.

$$K = \frac{k'}{k} \tag{8}$$

leading with Eqn. (7) to the relationship

$$T = T_1 - \frac{x_{0,2} \cdot R T_1^2}{\Delta H_{f,1}} \frac{1}{\frac{K}{1-K} + r} \tag{9}$$

The discussion of systems with eutectic impurities and impurities forming solid solutions is rather inconsistent.

With regard to this relationship, Driscoll *et al.* state: "Systems which form true solid solutions, however, cannot be handled by this method of analysis". Joy and coworkers[7] declare in their abstract: "Because the DSC technique is "blind" to equilibrium solid solution formation, DSC values should not be used as a sole criterion of purity". Mastrangelo and Dornte[8] reported on a mixture of 2,2-dimethylbutane and 2,3-dimethylbutane. These two substances are known to form solid solutions. Mastrangelo and Dornte find a reasonable agreement between the theoretical temperature relation of Eqn. (9) and the experimental findings.

We have found no complete experimental proof of Eqn. (9) in the literature. Such a proof would require the independent determination of the parameters and thermodynamic constants such as temperature T, mole fractions of the main component and the impurities, molten fraction r, the partition coefficient K, the melting point T_1, and the heat of fusion of the main component $\Delta H_{f,1}$. Investigations of this kind should result in an assessment of the equilibrium with respect to temperature and concentrations.

Reconsidering Eqn. (7), we find the limitation of this equation discussed by several authors with respect to the allowable concentration of impurities. The limit is not properly defined because the definition would require the introduction of an absolute deviation between the theoretical amount of eutectic impurities and the sum of eutectic impurities as determined by DSC. With the lack of such a definition it is not surprising that the limitation of Eqn. (7) is estimated with considerable differences: Davis and Porter[10] assumed a limitation of Eqn. (7), with respect to the concentration of eutectic impurities, of 5%; De Angelis and Papariello[11] assumed a limitation of 1%; and Joy *et al.*[7], one of 2%.

These limitations on the amount of eutectic impurities for the premelting method can be overcome by a method suggested by De Angelis and Papariello[11]. Samples of high impurity concentration (>1%) are diluted with the pure main component to extend the limit of the applicability of the DSC method. Such a dilution method was applied by De Angelis and Papariello to 4 different organic systems with actual purities of 95.5–97.0 mole-%. The DSC purity values of these samples without dilution gave results in a narrow range from 97.4 to 97.8 mole-%. The absolute differences between the true and the experimental purity values were, therefore, of the order of 1–2 mole-%. DSC results with such high inaccuracies are not sufficient for analytical purposes. The experiments of De Angelis and Papariello performed with the same compounds, but with a dilution of the main impurities with the corresponding main component to a purity level above 99 mole-%, resulted in excellent agreement between DSC values and the actual purity. Schumacher and Felder[12] present similar results in DSC purity values determined directly and after dilution with a substituted benztriazole as the main component.

The differences between the actual purity and the experimental values determined without dilution are explained by the authors of both papers[11,12] in terms of an inconsistency between Eqn. (7) and the actual melting behaviour of organic substances in a purity region below 99 mole-%. We found that such an explanation of the differences of theoretical and experimental purities appears to be, however, only one of several possibilities. Another possible explanation for the differences is that the DSC method without dilution, used by Papariello and Schumacher, is only applicable to substances with a purity of at least 99 mole-%. In contrary to the findings of Papariello and Schumacher, we observed for many substances that the method without dilution gave correct values for impurities in the case of samples with substantially higher concentrations of impurities. We found that highly accurate purity values can only be achieved by selecting a scan speed appropriate to both the impurity concentration and the evaluation procedure. Thus, using the simplest Perkin–Elmer type of evaluation[13], a scan speed of 0.625 °C min^{-1} will yield valid results only in the purity range above 98 mole-%. The accuracy of a melting curve evaluation is improved by a data collection and evaluation at more than the 5–7 points within the important melting region, as suggested by Perkin–Elmer[13]. The more sophisticated the data collection and evaluation, the less important are the experimental conditions—scan speed, weight of sample and sensitivity—for getting a purity value of a high accuracy.

If one observes differences between the experimental and the actual purity values one has to check the experimental conditions, including the type of sample pan used, the data collection, the evaluation procedure of the melting curve, and the melting behaviour of the substance. If after all these investigations the differences in the experimental and the actual purity persist, an inconsistency between Eqn. (7) and the melting behaviour of this specific system is highly probable.

The dilution method introduced by Papariello[11] is excellent for the solution of special problems. Its pratical use in an analytical laboratory is, however, limited by the amount of work involved. Therefore, the question of the limitation of the DSC method to a region of high purity substances (*e.g.* to a purity better than 98 mole-%) has to be reexamined because such a strong limitation would diminish the value of the whole method. Such an investigation of the purity region, in which the DSC method is a useful analytical tool, should be performed with binary systems. It would be very helpful if the phase diagrams of the selected binary systems were known from literature. With such a binary system, all kinds of possible parameters and conditions have to be varied; the ratio of the two compounds, the sample weight, the sample pan, the scan speed, the sensitivity, the first, second and following melting curves of the same sample if possible, and the data collection and evaluation. The results thus obtained may be discussed with respect to discrepancies between theoretical and experimental values of the purity, the heat of fusion, and the melting points. They can, moreover, reveal properties of the two components such as thermal stability, high vapor pressure in the melting region for one or both of the compounds, polymorphism, and anomalous behaviours demonstrated by the phase diagram and by the melting curve. Having completed these investigations on some binary systems one could perform a similar program on multi-component systems. All these results should give us information on the limitation of Eqn. (7).

(*b*) *Handling of the samples*

Gray[13] suggested the use of the volatile sample pan with an inside cover. This inside cover is made from aluminum to fit into the bottom part of the volatile pan. Driscoll *et al.*[6], Barral and Diller[14], Reubke and Mollica[15], and others regard the volatile sample pan with an inside cover as the best solution to avoid volatilization. The sample handling and the variation of the temperature treatment are most important for substances with polymorphism, in the presence of impurities with a high vapor pressure in the melting region of the main component, and with substances which are unstable in the melting region.

Difficulties also arise with the sample holders of the DSC-IB. The sample pans, the aluminum dome lids and the outside cover of the sample holders have to be carefully placed in the correct positions[14,16].

Barrall and Diller[14] make a good point on the preparation of samples whereby great care has to be taken in selecting test samples or in mixing of low concentration standards, because the sample size in DSC measurements has to be in the region of a few milligrams. For quantitative work with the DSC-IB, the sample size should be

between 1 and 5 mg. Results with a high reproducibility are only possible with special care in the handling procedure.

(c) *Calibration of the DSC apparatus*

The calibration of the temperature axis of the DSC with high purity standards should be performed in the way indicated by Barrall and Diller[14]. The calibration of the sensitivity of the DSC in calories per unit area presents no problems. Important for high purity measurements is the careful calibration of the thermal resistance between the sample pan holder and the sample pan with standards like indium, tin and lead; this is also shown in the interesting investigations performed by Barrall and Diller[14].

The question arises whether or not one is allowed to use inorganic materials as standards for the measurement of the thermal resistance, which can then be used in the purity determination of organic substances. However, the DSC-IB is nearly independent of the thermal resistance of the sample, as long as the sample consists of crystals of a rather small size[17].

(d) *Instrumental conditions for a purity determination*

The instrumental conditions for a purity determination are sensitivity or the calorimetric range, the scan speed, and the sample pan. There are mutual relationships between these experimental conditions and some of the properties of the instrumentation and the sample. As an exemple, the appropriate calorimetric range used in a purity determination depends on several conditions, *i.e.* heat of fusion of the main component, sample size, scan speed, concentration of impurities, and recording system or data collection.

The scan speed, as indicated in the literature[6,7,14], is in general kept at the lower end of the range, *i.e.* 0.625 or 1.25°C/min. Such low values of the scan speed are

TABLE III

EFFECT OF SAMPLE SIZE AND HEATING RATE ON CALCULATED PURITY (BARRALL AND DILLER[14])

Mixture	*Sample size (mg)*	*Heating rate (°C/min)*	*Purity (mole-%)*	
			Found[a]	*Known*[b]
Lead in tin	3.084	1.25	0.425	0.419
Lead in tin	3.084	5.0	0.185	0.419
Lead in tin	3.084	20.0	0.0828	0.419
Lead in tin	4.300	1.25	0.321	0.419
Lead in tin	6.284	5.0	0.857	1.16
Lead in tin	6.284	1.25	0.871	1.16
Lead in tin	6.284	0.625	0.899	1.16

[a]Calculated with partial areas considered to the vertex of the endotherm. [b]Determined by atomic absorption of lead with a Perkin–Elmer Model 303 spectrophotometer, using nitrous oxide as oxidizing agent to dissociate the tin compounds.

required for high purity measurements. Low values of the scan speed are necessary as the sample is probably not at thermal equilibrium during rapid rates of heating, according to Barrall and Diller[14]. The effects of sample size and heating rate on the measured purity in mixtures of lead in tin[14] are presented in Table III.

Three parameters are varied in Table III; sample size, scan speed, and purity level. The mixture with the lower concentration of lead seems to be strongly sensitive to changes of the heating rate with respect to the concentrations of lead calculated from melting curves. Conclusions from Table III are only typical for the applied conditions, such as the data collection and evaluation procedure. Generalizations are only possible after performing the investigations mentioned in part (*a*).

(*e*) *Evaluation of the melting curves*

The calibration of the instrument, the handling of the samples, and the determination of the correct instrumental conditions for obtaining a melting curve which may be easily handled by an evaluation procedure, are all possible with some care in the experimental work. However, understanding and performing the purity calculations from melting curves is rather complicated. Therefore, the literature about this subject is quite extensive. No review of evaluation methods is available in the literature.

A given procedure for the evaluation of a melting curve can be checked in several different ways; there are a great many internal and external checks possible. We will discuss here the external checks which are performed with the values resulting from a normal evaluation of a melting curve; *i.e.* (*i*) the melting point of the sample, (*ii*) the melting point of the pure main component, (*iii*) the heat of fusion of the pure main component, and (*iv*) the purity value of the sample. The melting point and the heat of fusion of the sample calculated by the evaluation procedure may be compared with the values measured directly on the melting curve by applying the calibration factors. The melting point and the heat of fusion of the pure main component can probably be found in the literature. Such literature values permit a comparison with the results from the evaluation of melting curves.

For test substances, the measured DSC purity value may be compared with the actual purity value known from mixing. A second method is to compare the DSC purity value with the purity information obtained from a separate analytical procedure. In the case of disagreement between the DSC purity value and the actual purity value, several points must be considered with regard to the DSC method; *i.e.* the instrumental conditions used in getting the melting curve; the physical and chemical behaviour of the main component and the impurities; and the evaluation procedure, and the use of the thermodynamic relationship for the description of the solid–liquid equilibrium.

All the considerations given in this section, which are necessary in case of discrepancies between the values evaluated from melting curves (*i.e.* purity, melting points, heat of fusion) and values found in the literature, receive practically no mention in the published work on DSC-purity determination.

The evaluation of melting curves by hand, suggested by Perkin-Elmer[13], is practicable but too cumbersome for routine work. Computer programs used in the evaluation give higher accuracies in purity and thermodynamic values, and are much faster. Programs were developed by Driscoll *et al.*[6], Scott and Gray[18], Barrall and Diller[14], Davis and Porter[10], Heuvel and Lind[19], Gent[20], and others.

The basic problems of the evaluation of melting curves by computer or by hand are the same. Referring to Eqn. (7), one has to fit the experimental DSC-curve to a straight line in the $(1/r, T)$-diagram, as it was first shown by Pitzer and Scott[21].

The evaluation procedures cited above consist of: (*1*) the fit of the experimental points from a melting curve to a given thermodynamic function, together with the determination of the true heat of fusion of the main component[6,10]; (*2*) the linearization with an appropriate mathematical method[6,18]; and (*3*) the calculation of the purity value and the thermodynamic constants of the sample and of the corresponding main component. It is not always possible to separate a given evaluation procedure into these three parts. However, the literature of the evaluation procedures is more easily discussed by such a partition.

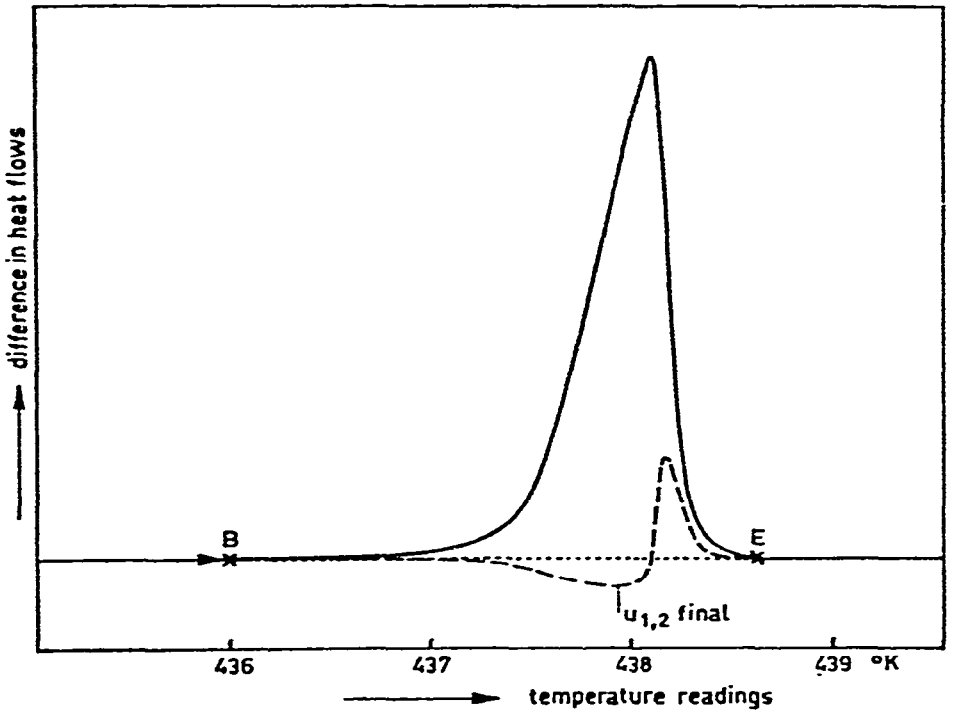

Fig. 2. Melting trace of benzanilide with a baseline $u_{1,2}$ *final* calculated by Heuvel and Lind[19].

The problem of evaluating the true heat of fusion exists because the DSC is measuring the difference in the heat necessary to maintain a given and constant temperature rise in the reference and the sample cell. The baseline of the instrument during an exothermic or endothermic change of the sample can only be determined

approximately by a connection of the recorder lines before and after such an energy change. Heuvel and Lind[19] stated, "Under certain conditions of instrument operation, *e.g.* fast scanning rates, the course of the base line deviates to a large extent from simple interpolation between pre-transition and post-transition baselines". Fig. 2 shows the melting trace of benzanilide from the paper of Heuvel and Lind. The indicated baselines are given by (*i*) a straight line from point B to E, and (*ii*) $U_{1,2}$ final; a function of the heating rate, the heat capacity of the sample, and the thermal resistance from the sample holder to the sample[17] according to the calculations of Heuvel and Lind[19].

For a sharp transition, as shown in Fig. 2, both baselines give the same calculated value for the heat of fusion, which is a conclusion of the paper of Heuvel and Lind[19].

The discussion of the heat of fusion is presented in two parts: (*1*) with high purity substances, and (*2*) with substances having lower purity values.

Table IV shows the heats of fusion for several high-purity substances. The values are directly calculated from melting curves in applying a straight baseline, as shown in Fig. 2.

TABLE IV

HEAT OF FUSION FROM DSC MELTING CURVES FOR SUBSTANCES OF A HIGH PURITY VALUE

Substances	*DSC purity (mole %)*	*Heat of fusion*		$\frac{\Delta H_{f,DSC}-\Delta H_{f,Lit.}}{\Delta H_{f,Lit.}} \times 100$ (%)
		DSC uncorrected baseline $\Delta H_{f,DSC}$ *(cal.mole*$^{-1}$*)*	*Lit. values* $H_{f,Lit.}$ *(cal.mole*$^{-1}$*)*	
Benzene	99.8	2352[a]	2349 (Ref. 22)	+0.1
Benzene	99.05	2237[a]	2349 (Ref. 22)	−4.8
Benzamide	99.25	4590[b]	4899 (Ref. 23)	−6.3
Benzoic acid		3945[b]	4300 (Ref. 24)	−8.3
Anthrachinon	99.94	7725[b]	7830 (Ref. 25)	−1.3
Potassium nitrate		2370[b]	2295 (Ref. 26)	+3.3
Distilled water	99.97	1400[b]	1434 (Ref. 27)	−2.4
Butazolidine	99.56 ±0.28[c]	5710[b] ±680[b,c]		

[a]DSC values by Driscoll *et al.*[6]. [b]DSC values by Marti and Heiber (unpublished). [c]Error in a single measurement on 95% confidence limits.

The agreement of the DSC with the literature values for the heat of fusion is reasonable in the case of high purity substances. The reproducibility of the heat of fusion, according to measurements on butazolidine, is indicative of a normal-precision, and certainly not of a high-precision instrument. A better precision in the determination of energies are expected from new instruments, *e.g.* Mettler DTA 2000[28] and Perkin–Elmer DSC-2[29].

The determination of the heat of fusion from melting curves of samples with low purity values reveals a completely different picture compared to that presented in Table IV. The results are presented in Table V. The measurements were performed by Driscoll *et al.*[6] for an impurity content of $\leqslant 2.80$ mole-%, and for highest value of impurities by a measurement in our laboratory. The determination of the heat of fusion was performed with an uncorrected baseline, as described in Fig. 2.

TABLE V

HEAT OF FUSION FROM DSC MELTING CURVES FOR BENZENE WITH VARIOUS AMOUNTS OF EUTECTIC IMPURITIES

Substance	*DSC purity (mole-%)*	*Heat of fusion DSC, uncorrected baseline* $\Delta H_{f,DSC}$ *(cal.mole*$^{-1}$*)*	$\frac{\Delta H_{f,DSC} - \Delta H_{f,Lit.}}{\Delta H_{f,Lit.}} \times 100$ (%)
Benzene	99.8	2352	+0.1
	99.05	2237	−4.8
	99.10	2131	−9.3
	97.14	1788	−23.9
	91.5	1293	−49.2

A correction of the heat of fusion for substances with purities below 99% is absolutely necessary. For example (see Table V, benzene, purity 91.5%), the eutectic impurity calculated in applying Eqn. (7) would be too low by as much as 50% for the theoretical impurity value of 8.5 mole-%. A similar picture of the difference between the heat of fusion according to the literature values and the DSC measurements was shown by Davis and Porter[10]. The difference in the values of the heats of fusion can be explained by (*i*) the fact that the instrument has a limited sensitivity, and (*ii*) a eutectic and premelting region which is unrecorded because the eutectic point may be far below the melting point of the main component.

The incorrect baseline measured by the DSC has not only an influence on the heat of fusion, but also on the evaluation procedure. The melting curve allows a calculation of the fraction of the substance melted as a function of temperature. The temperature indicated on the DSC-IB must be corrected to the temperature of the sample. The correction is performed with a temperature calibration curve of the instrument and with calibration measurements on the thermal lag between the sample holder and the sample[30]. The plot of the temperature of the sample as a function of the reciprocal molten fraction—the $1/r$, (T)-diagram—should give a straight line according to Eqn. (7). A straight line in the $(1/r, T)$-diagram can be observed occasionally for substances with an extremely high purity. All other substances give only a straight line after a trial and error correction of the baseline, the so callep linearization[13]. A new position of the baseline yields a new value of the heat of fusion. The linearization procedure corrects, at least partially, for the energy unrecorded

through the instrument's limitation and for the premelting region which is not observed. The linearization procedure leads to a more accurate determination of the heat of fusion of the main component.

The linearization in the $(1/r, T)$-diagram is only possible within a certain region of the melting curve. The limits of the linearization region are discussed in the paper by Driscoll *et al*[6]. They used for their linearization a constant value for the lower limit of the fraction melted with 2% and for the upper limit, a value based on the fraction melted at the point where the rate of heat input reaches half of its maximum value. This defines the upper limit from about 12.5% for a pure sample to about 40% for a sample with approximately 2 mole-% of eutectic impurities. The influence of the limits of the linearization interval on the calculated impurity values is shown in Table VI, taken from the work of Driscoll *et al.*[6].

TABLE VI

CALCULATED IMPURITY VALUES FOR NBS OCTANE WITH A CERTIFIED IMPURITY OF 0.06±0.04%

Linearization limits, fraction melted (%)		*Calculated impurity* (*mole-%*)
Lower limit	*Upper limit*	
2	10	0.016
2	18	0.23
2.5	36	0.52
2.5	40	0.59
2.5	50	0.78
10	50	2.69

Driscoll and coworkers emphasized the importance of the linearization limits, which are applied for the calculation of impurity values. Only with a comprehensive investigation on melting curves of substances which are close to an ideal melting behaviour, is one able to find proper values for the linearization limits. The necessity for an investigation of the linearization limits is clearly demonstrated in comparing the values of the linearization limits and the calculated impurities in Table VI. These calculated impurity values differ by two orders of magnitude from the NBS value.

In general, the performance of the linearization permits the calculation of the heat of fusion of the main component $\Delta H_{f,1}$; the melting point of the main component T_1, obtained from the intercept of the T-axis with the straight line of the corrected data for the melting curve in the $(1/r, T)$-diagram; and the melting point of the sample T_s as the temperature value where $r = 1$. The calculation of the eutectic impurity using Eqn. (7) can then be made without any difficulty.

Apart from the computing procedures for the determination of the concentration of eutectic impurity, there is another method suggested by Plato and Glasgow[31]. These two authors reported their experiences with 95 different organic compounds analyzed with the DSC: "An experienced analyst can estimate the purity of an

unweighed sample to within about 0.2 mole-% by visual inspection of the DSC curve produced in a 3-min scan". This remark can be regarded as the introduction of a new evaluation method. However, this new evaluation method of melting curves would demand, in our opinion, the following procedure, especially to reach the goal of an accuracy in eutectic impurities of ±0.2 mole-%: (*1*) Preparation of a set of reference melting curves; the range of eutectic impurities and the instrumental conditions required to set up reference curves should be appropriate to the samples which have to be measured for analytical purposes. (*2*) Measurement of the melting curves of samples with the same instrumental conditions as used for the reference curves. (*3*) Comparison of the melting curves and the reference curves. Using the improved method of Plato and Glasgow the computer program for the calculation of purity values can be partially replaced.

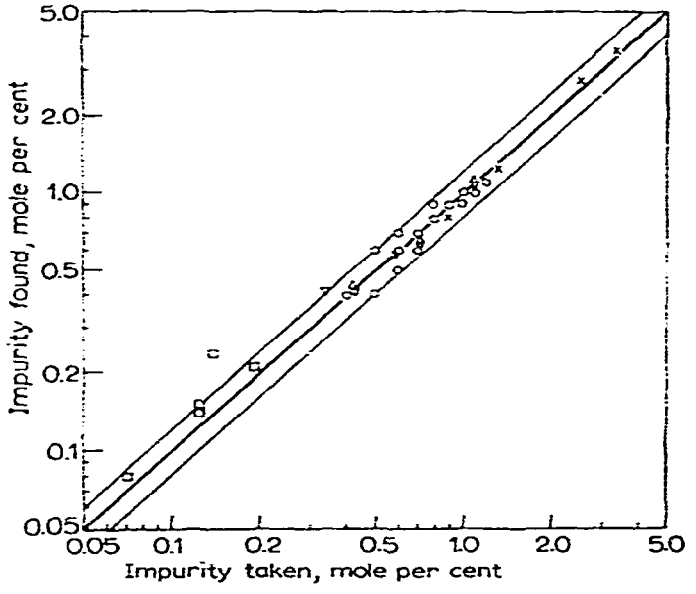

Fig. 3. Relation between actual and experimental impurity value (Joy *et al.*[7]).

(f) Accuracy of measurements of eutectic impurities with DSC

All authors agree that the accuracy of the impurity values measured with DSC decreases with increasing content of eutectic impurities. Barrall and Diller[14] claim a high relative accuracy of ±3% with respect to the eutectic impurity, but only in case of high-purity substances. Reubke and Mollica[15] reported on substances in the purity region of 99 to 100%. These authors claim an absolute error in the eutectic impurities of 0.1%, which means more than 10% relative to the amount of impurities. Joy and coworkers[7] make the interesting remark that the upper limit in purity measurements with DSC are 99.95 mole-%. Higher numerical values of the purity seem to bear no significance. The statement of Joy and coworkers of the existence of an absolute error in eutectic impurities of only 0.05 mole-% is quite close to the value given by Reubke and Mollica. This minimum value of the absolute error of the

impurity measurements is of course typical for the DSC-IB. An extensive comparison of theoretical and measured DSC values is presented in Fig. 3. The substances are selected by Joy *et al.* and the purity of most of these substances is in the region of $99.0 \pm 0.5\%$.

The upper and lower lines on the graph indicate the +20% and −20% relative error limit. It should be added, however, that only substances with no problems in melting (*e.g.* suspected solid solution formation, incomplete solubility of the impurities in the melt, or other disturbances) were chosen by Joy for presentation in Fig. 3. De Angelis and Papariello[11] give examples of organic substances with absolute errors between the actual and DSC purity values of 0.5 mole-% at the 98-% purity level and 2.5 mole-% at the 95-% level. The actual values of the purity are given by dry mixing the main component and the impurity. Dry mixing of substances in the purity range of less than 99% should be without any problems. Therefore actual values of the purity known from mixing of the main component and impurities are expected to be very close to the true purity values. The relative accuracies of eutectic impurities, according to the measurements and calculations of De Angelis and Papariello, are within 25% for the 98-% purity level and 50% for the 95-% level. De Angelis and Papariello explain, "We have not yet encountered any system in which accurate results were obtained beyond 1.5 mole-% impurity and it is indicated that DSC purity values of less than 99% are likely to be in error". From statements in the literature on accuracy in the determination of eutectic impurities the following conclusion can be made. There are two regions of purity with an arbitrary separation limit of 99 mole-%. The probability of a good agreement of actual and measured impurity values is high in the high-purity region, and low in the low-purity region. A first step to a clearer situation in the low-purity region could be reached by an extensive study on any system which shows great differences in actual and experimental purity values.

(*g*) *Application of the purity determination to substances which are unstable in the melting region*

Reubke and Mollica[15] reported, "Samples were selected which would melt without decomposition". Plato and Glasgow[31] stated, "Purity of chemicals that decompose near their melting points cannot be determined by the DSC method". Throughout the literature one can find the statement that the DSC method is unable to handle substances which decompose during melting.

THEORY OF THE PURITY DETERMINATION USING THE METHOD OF PREMELTING ON BINARY SYSTEMS WITH A EUTECTIC PHASE DIAGRAM

The theory of the purity determination with the method of premelting was discussed by Marti *et al.*[32] for a binary system with a eutectic phase diagram. A binary system is the simplest system for a theoretical discussion of the purity determination by DSC, also for experimental work it is easy to collect all the necessary information from the literature or by measurements. The understanding of the

melting behaviour of a binary system from a theoretical and experimental point of view is certainly the most important part of the attempt to understand the melting behaviour of a multicomponent system.

The melting behaviour of a eutectic system consisting of only two components is commonly described approximately by a thermodynamic relationship in the region of solid–liquid equilibria. Such a description is given in Eqn. (10)[33] for an ideal mixture of non-electrolytes under isobaric conditions with a heat of fusion independent of temperature.

$$\ln (x_i) = \frac{\Delta H_{f,i}}{R}\left(\frac{1}{T_i} - \frac{1}{T}\right) \qquad (i = 1, 2) \tag{10}$$

where x_i is the mole fraction of the component i in the liquid phase, $\Delta H_{f,i}$ is the heat of fusion of the pure component i at the melting point, R is the gas constant, T_i is the melting point of the pure component i in °K, and T is the temperature in °K.

The mole fractions for a binary mixture are connected by the equation

$$x_1 + x_2 = 1 \tag{11}$$

At low values of one of the components, *e.g.* component 2, we can write Eqn. (10) in the form

$$x_2 = \frac{\Delta H_{f,1}}{R}\left(\frac{1}{T} - \frac{1}{T_1}\right) \tag{12}$$

More exactly, the solubility equilibrium (Eqn. 10) is found by introducing a heat of fusion, ΔH_i, which is a function of temperature[34]. In this case we can write

$$\Delta H_i = \Delta H_{f,i} + \Delta C_{0,i}(T - T_i) \tag{13}$$

where $\Delta C_{0,i}$ is the difference of the molar heat capacities of the pure component i at constant pressure for the liquid and the solid phase.

Eqn. (13), applied to the solubility equilibrium of an ideal mixture, leads to the following relationship

$$\ln (x_i) = \frac{\Delta H_{f,i}}{R}\left(\frac{1}{T_i} - \frac{1}{T}\right) - \frac{\Delta C_{0,i}}{R}\left(1 - \frac{T_i}{T} + \ln \frac{T_i}{T}\right) \tag{14}$$

The following abbreviation will be used for Eqn. (14)

$$\ln (x_i) = \mathrm{A}(T) \tag{15}$$

Eqns. (10), (12) and (14) enable us to construct the isobaric melting point diagram for binary systems, which are ideal mixtures on the basis of the properties of the main components alone (namely melting points, heats of fusion, and heat capacities).

A mixture of phenacetin and benzamide was chosen as an example of a binary system. The thermodynamic values used for the calculation of the phase diagram are given in Table VII.

TABLE VII
THERMODYNAMIC PROPERTIES OF PHENACETIN AND BENZAMIDE

Thermodynamic values	*Phenacetin*		*Benzamide*	
	Author's values by DSC	*Lit. values*	*Author's values by DSC*	*Lit. values*
Melting point T_t (°K)	407 ±0.3	407–408[35]	400 ±0.3	400–400.7[36]
Heat of fusion $\Delta H_{f,t}$ (cal/mole)	7750 ±600	7880[a]	4900 ±600	4900[37]
Difference between the molar heat capacities in the liquid and the solid phase $\Delta C_{p,t}$ (cal/mole °K)	12.5 ±0.5		13.3 ±0.5	

[a]Calculated from the heat of sublimation ($\Delta H_s = 27.60$ kcal mole^{-1})[38] and the heat of evaporation ($\Delta H_v = 19.72$ kcal mole^{-1})[39].

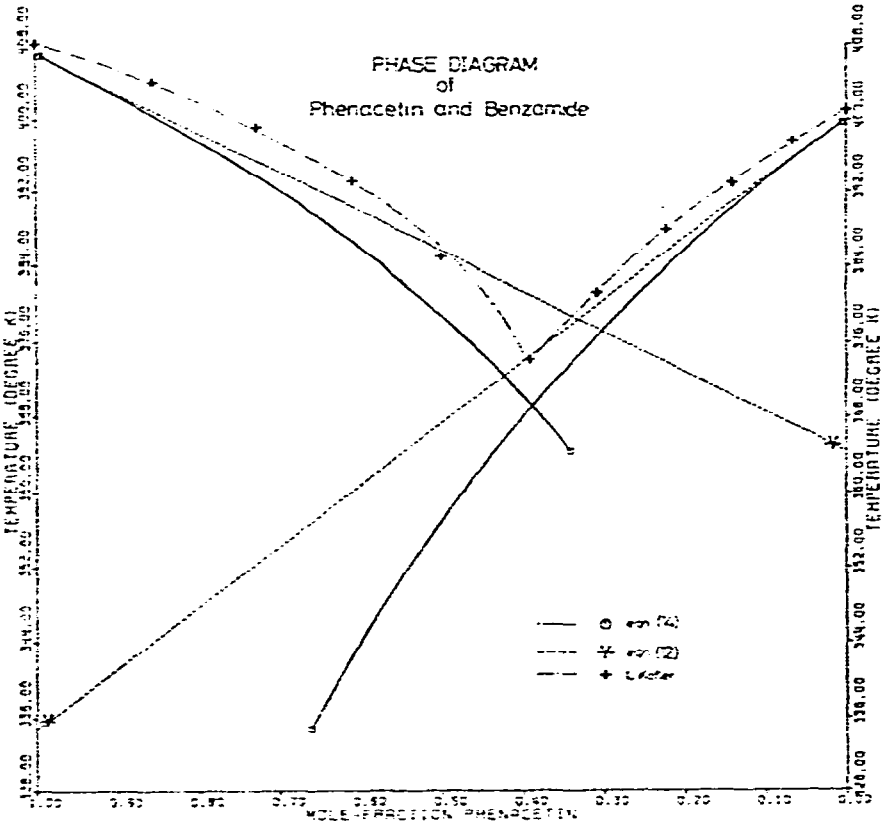

Fig. 4. Comparison of theoretical and experimental phase diagrams for phenacetin and benzamide (Kofler, Marti *et al.*[32]).

In Fig. 4, the melting point diagrams calculated from Eqns. (12) and (14) are compared with a diagram from measurements by Kofler[40]. The differences between the two theoretical phase diagrams are easily understood by the two levels of approximation applied to Eqns. (12) and (14). However, the differences between the theoretical

phase diagram calculated with Eqn. (14) and the experimental phase diagram are certainly caused by the difference between the activities of the components, and the concentration itself. A smaller part of the differences may be due to experimental conditions. A discussion of the activity can be attempted by introducing the relation[41]

$$a_i = x_i f_i \tag{16}$$

where a_i is the activity of the component i in the liquid phase, and f_i is the activity coefficient of the component i.

The activity coefficient, f_i, of a binary liquid mixture of non-electrolytes is defined by Eqn. (17)

$$\mu_i = \mu_i^\circ + RT \ln (x_i f_i) \qquad (i = 1, 2) \tag{17}$$

where μ_i is the chemical potential of component i in the liquid phase and μ_i° is the chemical potential of pure liquid component i at the same pressure and temperature.

A relationship exists between the activity coefficients f_1 and f_2 because of the mutual interaction of the substances in a binary system and because of the equilibrium between the phases of a heterogeneous system. The equilibrium condition demands that all the phases must have the same temperature T, the same pressure P, and the chemical potential of each component must have the same value of μ_i in all the phases.

The relationship between the activity coefficients follows from a combination of Eqns. (11) and (17) and in the application of the Gibbs–Duhem relationship

$$x_1 \left(\frac{\delta \ln f_1}{\delta x_1}\right)_{T,P} + (1 - x_1) \left(\frac{\delta \ln f_2}{\delta x_1}\right)_{T,P} = 0 \tag{18}$$

The activity coefficient f_i is a function of temperature, pressure and the mole fraction of the components; it is determined by a solubility measurement of each component at the temperature T and at isobaric conditions according to Eqn. (19), which follows from Eqns. (14) and (16)

$$\ln (x_i f_i) = \frac{\Delta H_{f,i}}{R} \left(\frac{1}{T_i} - \frac{1}{T}\right) - \frac{\Delta C_{0,i}}{R} \left(1 - \frac{T_i}{T} + \ln \frac{T_i}{T}\right) \tag{19}$$

The point-to-point determination of the activity coefficient is cumbersome. The problem may be solved relatively easily if we can specify the form of the function of the activity coefficient $f_1 (T, x_1)$. This function is then found, to a certain approximation, by combining only a few solubility data from Eqn. (19) along with the temperature dependence of the activity coefficient. The temperature dependence at a given concentration x_1 is related to the temperature dependence of the chemical potential by

$$\left(\frac{\delta \ln f_1}{\delta T}\right)_{P,x_1} = -\frac{\Delta H_1^*}{RT^2} \tag{20}$$

where ΔH_1^* is the differential heat of mixing given by the following equation

$$\Delta H_1^* = H_1 - H_1^0 \tag{21}$$

where H_1^0 is the molar enthalpy of the pure liquid component 1 and H_1 is the partial molar enthalpy of component 1 in the mixture.

With the determination of the function $f_1(T, x_1)$ from measurements on a binary system, the function $f_2(T, x_2)$ is also known according to Eqn. (18). Each branch of the melting point diagram of a binary system under isobaric conditions is described to a good approximation by Eqn. (19) and the thermodynamic constants of the corresponding main component known from the literature or from the measurements of heat of fusion, melting point, difference of the molar heat capacities for the liquid and the solid phase, and the activity coefficient.

Next, theoretical melting curves for different values of the ratio of the components for a given binary system are calculated. The calculation is based on the Eqns. (12) and (14) under the restriction to ideal mixtures. A melting curve can be defined by the rate of heat flow to the sample which, in a solid–liquid equilibrium, is a function of the temperature. The melting curve is further dependent on the ratio of the components and on the phase diagram of the binary system. Such a representation of the melting curves by the rate of heat flow as a function of temperature is experimentally obtained by the DSC method. In contrast to the paper by O'Neill[17], which presents a fusion analysis with the rate of heat flow, our discussion of the melting curves is based on the specific heat function. The relation between rate of heat flow, specific heat function and scan speed is given in Eqn. (22)

$$\frac{dH}{dT} = \frac{dH}{dt} \cdot \frac{dt}{dT} \tag{22}$$

where dH/dT is the specific heat function at constant pressure (cal $°K^{-1}$ $mole^{-1}$), dH/dt is the rate of heat flow (cal sec^{-1} $mole^{-1}$), and dT/dt is the scan speed in $°K\ sec^{-1}$. There is no difference, in principle, in discussing the melting behaviour with the rate of heat flow or the specific heat function.

One branch of the phase diagram is selected with the condition for component 2 of

$$x_{0,2} < x_{e,2} \tag{23}$$

where $x_{0,2}$ is the mole fraction of component 2 in the binary mixture and $x_{e,2}$ is the mole fraction of the component 2 at the eutectic point.

The condition in Eqn. (23) defines component 1 as the main component of the mixture. The eutectic melting at the eutectic temperature T_e is neglected by setting the temperature limits for Eqns. (12) and (14)

$$T_1 > T > T_e \tag{24}$$

The relation between the mole fraction x_2 of component 2 in the liquid phase and the mole fraction of this component in the given system ($x_{G,2}$) is

$$x_2 = \frac{x_{0,2}}{r} \tag{25}$$

where r is the molten fraction of the mixture.

By inserting Eqn. (25) into the equation for the solubility equilibrium in Eqn. (12), we obtain

$$\frac{x_{0,2}}{r} = \frac{\Delta H_{f,1}}{R} \cdot \left(\frac{1}{T} - \frac{1}{T_1}\right) \tag{26}$$

The introduction of the molten fraction r enables us to write the specific heat function as

$$\frac{dH}{dT} = \frac{dH}{dr} \cdot \frac{dr}{dT}. \tag{27}$$

The derivative dr/dT is calculated from Eqn. (26). The other derivative dH/dr can be formed using the following relation

$$H_r = \Delta H_{f,1} \cdot r \tag{28}$$

The relation in Eqn. (28) holds because of the limitation to eutectic systems and because of the restriction to ideal mixtures. Insertion of dH/dr and dr/dT into Eqn. (27) leads to the specific heat function

$$\left(\frac{dH}{dT}\right)_1 = x_{0,2} \frac{RT_1^2}{(T_1 - T)^2} \tag{29}$$

The integration of Eqn. (29) can be performed between the limits T_a and $T_{s,1}$

$$\int_{T_a}^{T_{s,1}} \left(\frac{dH}{dT}\right)_1 dT = x_{0,2} \cdot RT_1^2 \int_{T_a}^{T_{s,1}} \frac{dT}{(T_1 - T)^2} \tag{30}$$

The upper limit $T_{s,1}$ is the melting point of the given mixture and is approximated [see Eqn. (26), $r = 1$] by

$$T_{s,1} = T_1 - x_{0,2} \cdot \frac{RT_1^2}{\Delta H_{f,1}} \tag{31}$$

The lower limit is more or less arbitrarily chosen as

$$T_a = T_1 - \frac{RT_1^2}{\Delta H_{f,1}} \tag{32}$$

defining r as equal to $x_{0,2}$ for this lower limit.

The definition of the lower limit of the specific heat functions excludes the energetic change of binary systems at the eutectic points. There is no continuity between the eutectic point and the melting region which would demand a mutual discussion of both phenomena.

By repeating the procedure, which gave Eqn. (29) from Eqn. (26), with the solubility equilibrium from Eqn. (14) we obtain the specific heat function

$$\left(\frac{dH}{dT}\right)_1 = \frac{x_{0,2}}{RT^2} \cdot [\Delta H_{f,1} + \Delta C_{0,1}(T - T_1)]^2 \cdot \frac{1}{e^{A(T)} + e^{-A(T)} - 2} \tag{33}$$

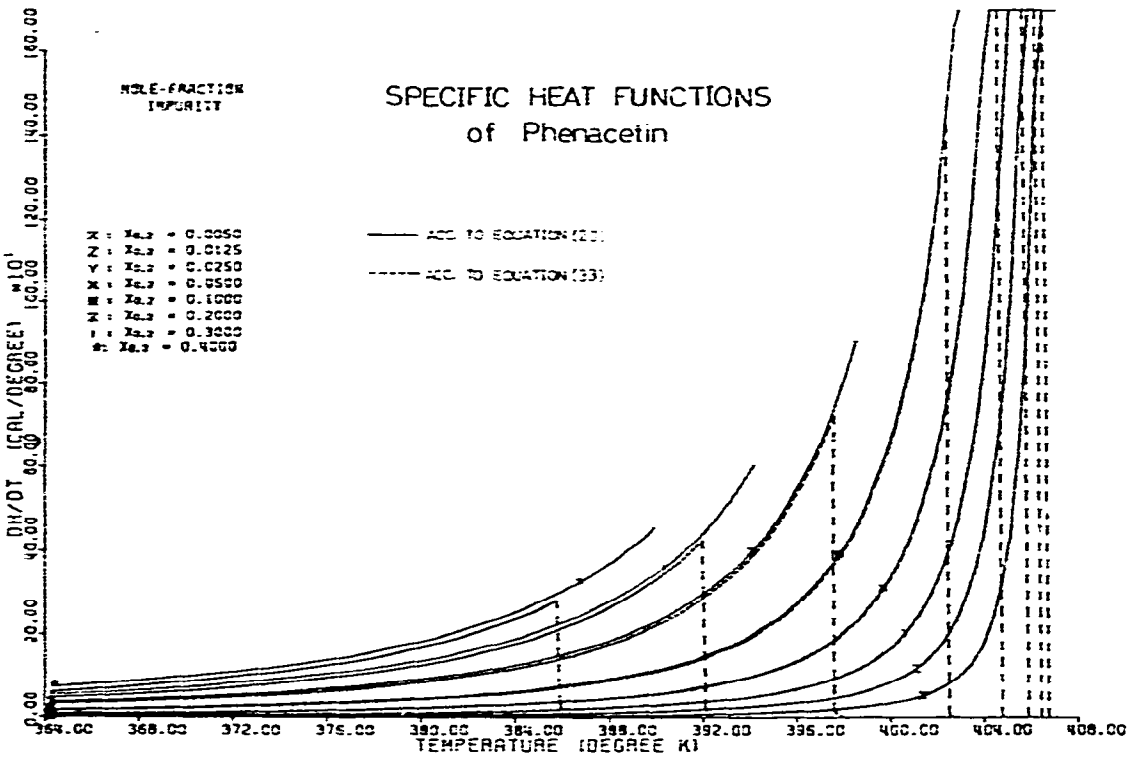

Fig. 5. Specific heat functions of phenacetin from Eqns. (29) and (33).

For a given mole fraction, the theoretical specific heat functions according to Eqns. (29) and (33) depend only on the properties of the main components. Specific heat functions of phenacetin and benzamide are presented in Figs. 5 and 6. The sets of specific heat functions for phenacetin are calculated according to Eqns. (29) and (33), whereas for benzamide, only one set of curves from Eqn. (29) is shown. The thermodynamic values of the main components used for our calculations are shown in Table VII. The following mole fractions of component 2 (impurity) were used for the presentation of the specific heat functions in the case of phenacetin and benzamide; $x_{0,2} = 0.005$, 0.0125, 0.025, 0.05, 0.10, 0.20, 0.30. In addition, for phenacetin as the main component, a curve with $x_{0,2} = 0.40$ was also plotted. The upper and lower limits of the specific heat functions calculated according to Eqn. (29) are determined by Eqns. (31) and (32). In Figs. 5 and 6, the curves are plotted between these limits if the selected range of the specific heat of 1600 cal $°K^{-1}$ allows such a presentation. As

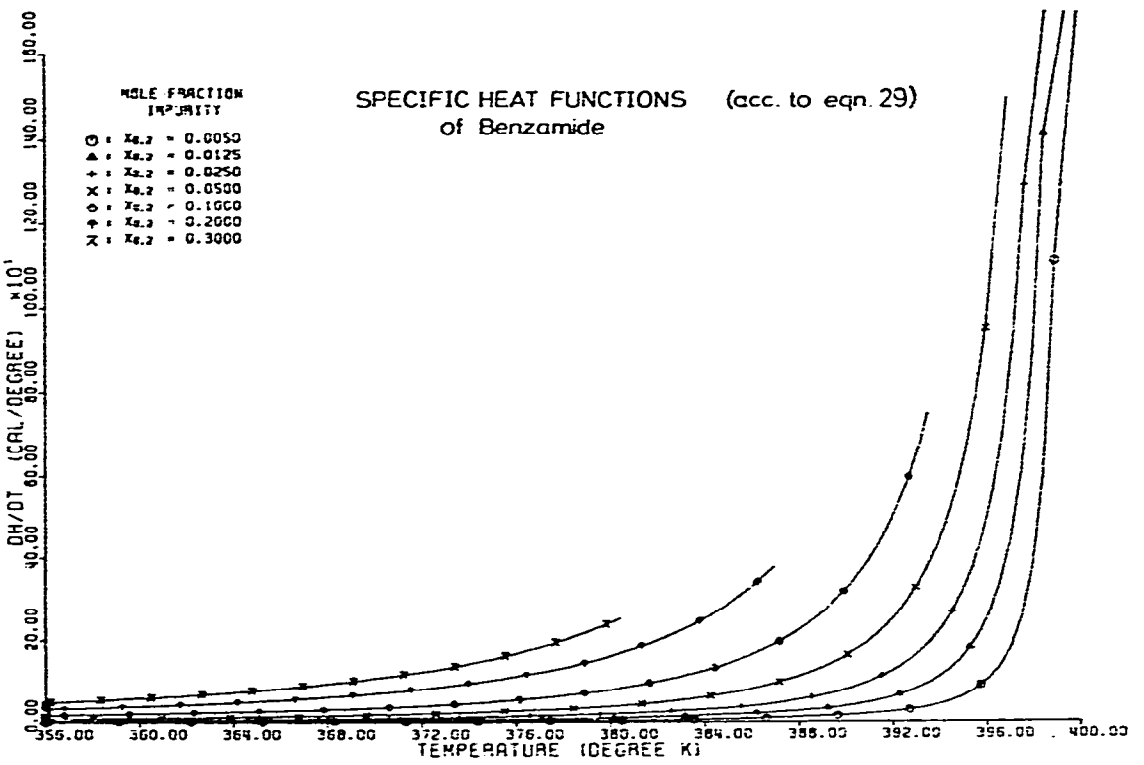

Fig. 6. Specific heat functions of benzamide from Eqn. (29) (Marti *et al.*[32]).

an example, a comparison of the specific heat functions for phenacetin and benzamide with a mole fraction of component 2 ($x_{0,2} = 0.3$) shows differences caused mainly by the difference in the melting points and the heat of fusions. Among other subjects, there is an investigation in a subsequent part of this paper into the difference of specific heat functions calculated using Eqn. (29) for main components which differ in their thermodynamic constants.

The differences of the specific heat functions from Eqns. (29) and (33) are shown in Fig. 5. Significant differences between the specific heat functions (shape of curves and upper limits) are only seen for extremely high impurity values (component 2). For the specific heat functions of Eqn. (29) the upper limits (melting points) were evaluated from Eqn. (31). Eqn. (31) is only a poor approximation in a region of the mole fraction of component 2 between 0.4 and 0.1. The absolute values and relative differences of the specific heat functions of phenacetin as main component, calculated from Eqns. (29) and (33), are presented for selected temperature values and mole fractions in Table VIII.

The relative differences of the specific heat functions calculated with Eqns. (29) and (33) are strongly dependent on temperature but are practically independent of the mole fraction of the main component. Table VIII clearly shows that the differences in the assumptions used for the calculation of specific heat functions are not really

TABLE VIII

COMPARISON OF SPECIFIC HEAT FUNCTIONS CALCULATED FROM EQN. (29) OR EQN. (33)

Temperature	*Mole fraction of component 2*	(dH/dT) *from Eqn. (29)*	(dH/dT) *from Eqn. (33)*	$\frac{(dH/dT)_{29}-(dH/dT)_{33}}{(dH/dT)_{29}} \times 100$
364.3	0.30	54.4	46.0	15.5
391.8	0.30	428.2	412.8	3.8
364.3	0.05	9.1	7.7	15.4
391.8	0.05	71.5	68.9	3.6

essential for the shape of the curves and, therefore, calculated impurity values in mole fractions change only a little when using either Eqn. (29) or (33).

It is even possible to go one step further in saying that to a certain approximation the specific heat function is only dependent on the mole fraction of the second component (impurity) as long as the restriction of eutectic systems holds. To explain this statement and to show the closeness of this approximation, Eqn. (29) may be written in the transformed form

$$\left(\frac{dH}{dT}\right)_1 = x_{0,2}\frac{R}{1-2\frac{T}{T_1}+\left(\frac{T}{T_1}\right)^2} \tag{34}$$

Now, two mixtures with different main components and melting points of the pure substances T_1 and T_2, respectively can be compared. The following temperature difference, ΔT, is introduced

$$\Delta T = T_2 - T_1 \tag{35}$$

The specific heat function of mixture number 2 is represented on a shifted scale, namely

$$T' = T - \Delta T \tag{36}$$

The specific heat functions are indicated with the indices 1 and 2 and the mole fraction of the impurity in both cases is made the same. The ratio of the two specific heat functions formed with Eqn. (34) can be written as

$$\frac{\left(\frac{dH}{dT}\right)_1}{\left(\frac{dH}{dT}\right)_2} = \frac{1}{\left(1+\frac{\Delta T}{T_1}\right)^2} \tag{37}$$

Obviously, the ratio of the specific heat functions taken at corresponding temperatures is constant.

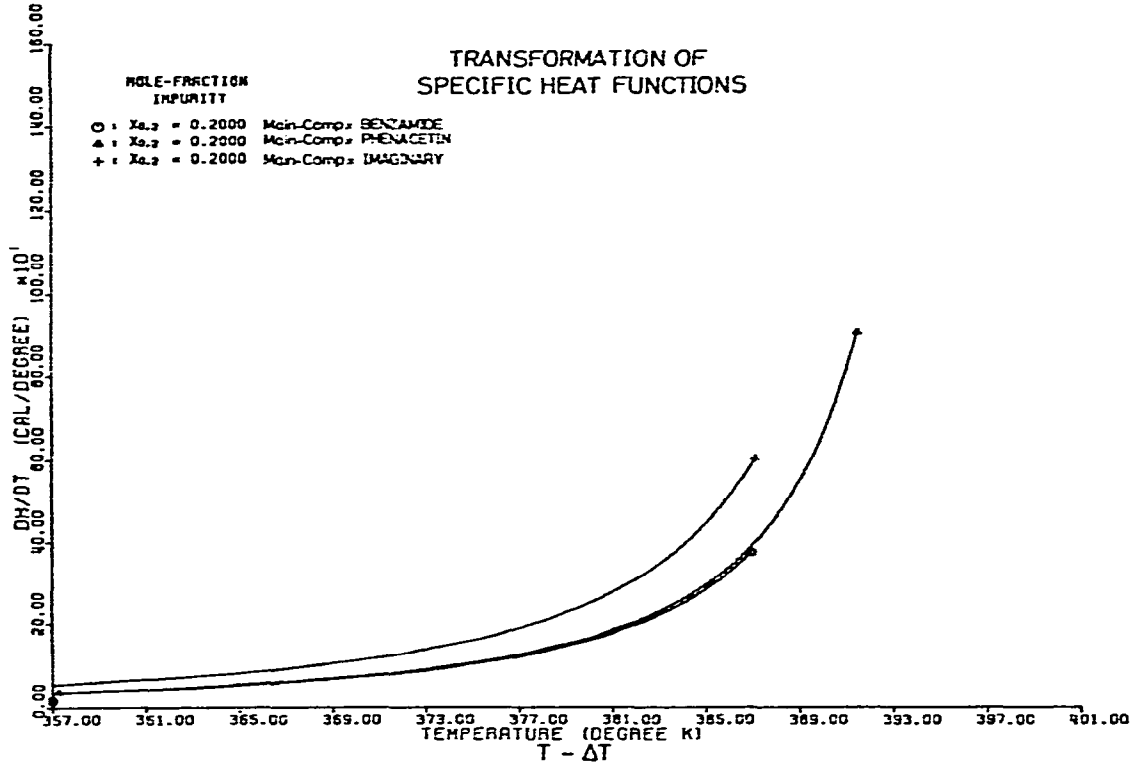

Fig. 7. Transformation of specific heat functions (Marti *et al.*[32]).

As an example, three specific heat functions on a transformed temperature scale are represented in Fig. 7 with a constant mole fraction $x_{0,2} = 0.2$. The substances and thermodynamic values used in these examples are shown in Table IX.

TABLE IX

THERMODYNAMIC PROPERTIES OF THE COMPOUNDS USED FOR FIG. 7

Substance	*Heat of fusion* $\Delta H_{f,1}$ *(cal/mole)*	*Melting point* T_1 *(°K)*	*Temp. shift* T *(°K)*
1. Benzamide	4900	400	0
2. Phenacetin	7750	407	7
3. Imaginary substance	7750	500	100

Eqn. (37) and the values in Table IX give the ratios

$$\frac{\left(\frac{dH}{dT}\right)_1}{\left(\frac{dH}{dT}\right)_2} = 0.966 \quad \text{and} \quad \frac{\left(\frac{dH}{dT}\right)_1}{\left(\frac{dH}{dT}\right)_3} = 0.64$$

which agree fully with the ratios taken directly from the specific heat functions in Fig. 7.

A second point observed in Fig. 7 is the position of the upper limit of the specific heat functions. This limit is given by Eqn. (31) and, for a constant mole fraction of the impurity, depends only on the cryoscopic constant of the main component.

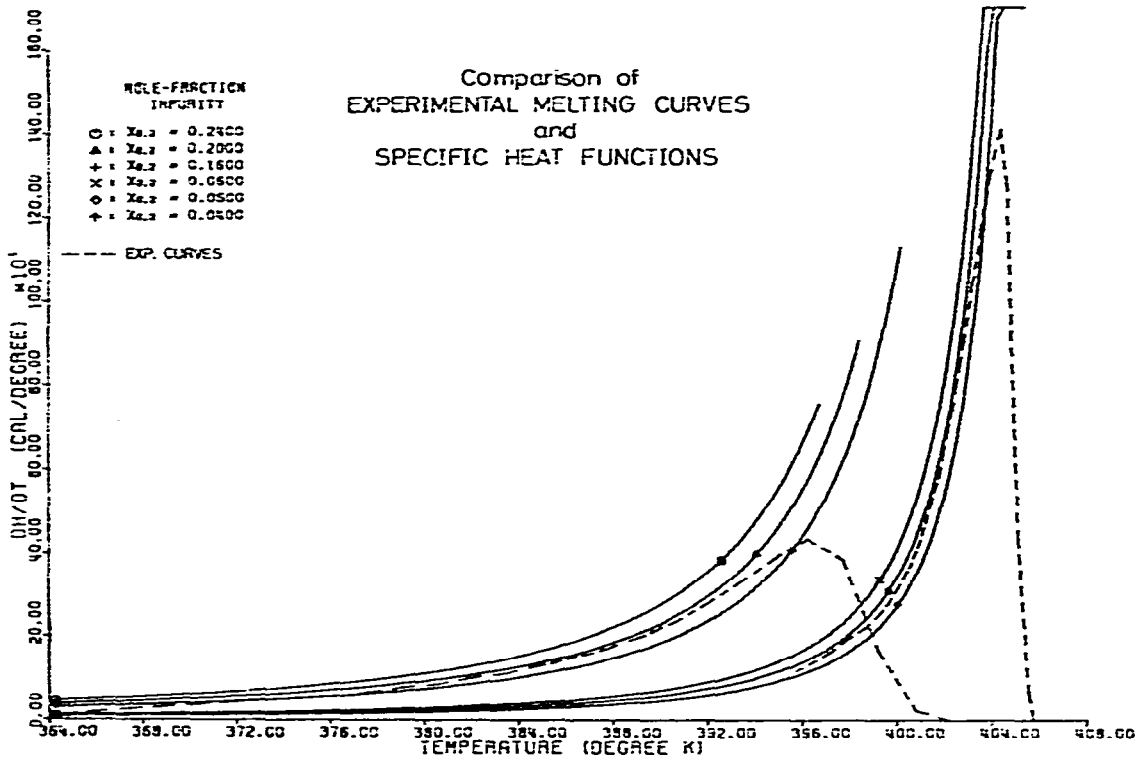

Fig. 8. Comparison of experimental melting curves and specific heat functions for phenacetin as main component and benzamide as impurity (Marti *et al.*[32]). The actual impurity values in mole fraction of the two mixtures are $x_{0,2}^{exp} = 0.2$ and 0.05.

In Fig. 8, theoretical specific heat functions for phenacetin calculated with Eqn. (29) and experimental curves recorded with the DSC-IB instrument of the Perkin–Elmer Corp. are compared. The samples were carefully mixed from phenacetin OAS (main component) and crystalline benzamide (impurity). The purities of both components used for the preparation of the mixtures were determined with the DSC-IB and evaluated with a computer program. The mean values of eutectic impurities of the two components are: phenacetin OAS, 0.25 ± 0.05 mole %; benzamide cryst. 0.66 ± 0.10 mole %.

The mixtures under investigation can be regarded as pseudo-binary systems with components of such a purity level, especially for the chosen mole fractions of the components. In Fig. 8, the experimental curves for $x_{0,2} = 0.2$ and 0.05 (concentration

of the impurity) are presented after transforming the ordinates $Y_{exp.}$ with a factor f_{DSC} to reach the same scale as applied for the theoretical curves.

$$Y = Y_{exp.} \cdot f_{DSC} \tag{38}$$

The factor is determined by the equation

$$f_{DSC} = \frac{B}{\dot{T}} \cdot R_f \cdot \frac{M}{m} \tag{39}$$

where B = recorder speed (cm min^{-1}), $\dot{T}$ = scan speed (°K min^{-1}), R_f = range factor (cal cm^{-2}), M = molecular weight of the main component (g), and m = sample weight of main component (g).

The temperature scale was only shifted according to a temperature calibration curve used for the measurements with the DSC-IB. No correction of the experimental curves for the thermal resistance of the DSC instrument were applied. Correction is certainly necessary for tan α values (thermal resistance) of less than 20.

The experimental conditions for the melting curves presented in Fig. 8 are as follows:

Mole fraction of benzamide	*Sample weight (mg)*	*Range (mcal sec^{-1})*	*Scan speed (°K min^{-1})*
0.2	3.09	4	16
0.05	3.20	4	4

Fig. 8 shows the agreement between the theoretical and experimental curves at least for the important melting region used for the determination of purity values.

DISCUSSION OF THE MEASUREMENTS OF SYSTEMS WITH IMPURITIES FORMING SOLID SOLUTIONS WITH THE MAIN COMPONENT

The two basic forms of phase diagrams are eutectic systems and systems with a complete range of solid solutions. One observes, normally, in the region of low concentration of one component either the form of a eutectic system or a solid solution. All other effects are restricted mainly to a mole-fraction region from about 0.1 to 0.9. As an example one is unlikely to find a congruently- or incongruently-melting compound in the concentration range of 0–0.1.

A theoretical representation of the melting curves for systems of solid solutions is not as easy as in the case of substances with a eutectic phase diagram. This difficulty arises because the concentrations of the components are normally a function of temperature, (*i*) in eutectic systems only in the liquid phase, and (*ii*) in systems of solid solutions in the liquid phase as well as in the solid phase. We shall now discuss a

temperature change for a eutectic system and a system of a solid solution within the temperature region of the solid–liquid equilibrium.

A system at equilibrium conditions at a given temperature is brought to a non-equilibrium condition by an infinitely-fast temperature change. The system will recover from these non-equilibrium conditions with two relaxation processes, a heat flow and a mass transport. The mass transport is caused by the temperature change and, therefore, the mass transport is consecutive to the heat flow. Equilibrium concentrations of the components are attained anew by diffusion of the components inside the phase. In eutectic systems, the diffusion is restricted to the liquid phase. In systems of solid solutions the diffusion of components occurs in the liquid and in the solid phase. The difference in the relaxation processes for eutectic systems and systems of solid solutions is mainly due to the difference in the diffusion rates in the liquid or in the solid phase. Therefore these diffusion rates which determine the relaxation times differ in order of magnitude.

Another difficulty in systems of solid solutions is caused by the crystallization of the substances. The crystallization conditions have an influence on the crystals formed. The solid phase may consist of so-called "zone crystals", which differ according to the conditions of crystallization in their concentration profile over cross-sections of any single crystal. Melting curves of zone crystals, which are measured at different non-equilibrium conditions are influenced by the actual concentration profile of the crystals.

Investigations into equilibrium or non-equilibrium conditions during the melting of systems of solid solutions are important for a similar treatment of purity determination in eutectic systems and systems of solid solutions. A similar purity determination for systems of solid solutions does not exist on the same level as in the case of eutectic systems.

The systems of solid solutions are only discussed phenomenologically and the possibilities of the DSC method are explained for a specific system, namely benzene–thiophene. The measurements published by Driscoll *et al.*[6] on benzene–thiophene are presented in Table X. The measurements were made on a pseudobinary system, of

TABLE X

DSC MEASUREMENTS OF SOLID SOLUTIONS IN THE BENZENE–THIOPHENE SYSTEM BY DRISCOLL *et al.*[6]

Sample	*Impurity*	*Added impurity (mole-%)*	*True impurity (mole-%)*	*Measured impurity (mole-%)*	ΔH_f *(cal/mole)*
Benzene	Thiophene	0		0.11	2352
		0.07	0.18	0.21	2209
		0.20	0.31	0.13	2364
		0.44	0.55	0.13	2370
		1.27	1.38	0.30	2438
		3.04	3.15	0.43	2291
		5.27	5.38	0.97	2468

benzene and thiophene. These two compounds are known to form solid solutions. The added impurity in Table X refers to thiophene. The true impurity is the added impurity (thiophene), corrected with the eutectic impurity (benzene), and could be measured with the DSC if benzene and thiophene could form a eutectic system.

The measured impurity, the impurity of benzene, and the heat of fusion of the samples were determined with the DSC apparatus. The measured impurity is only about 13% of the value of the true impurity, at least for the addition of more than 1 mole-% of thiophene. From the investigations by Driscoll *et al.*, one can calculate a distribution ratio of the impurity between the solid and the liquid phase of about $K \approx 4$. The calculation is, of course, only a rough approximation. We do not know if the distribution ratio is a function of the conditions prevalent during the measurements.

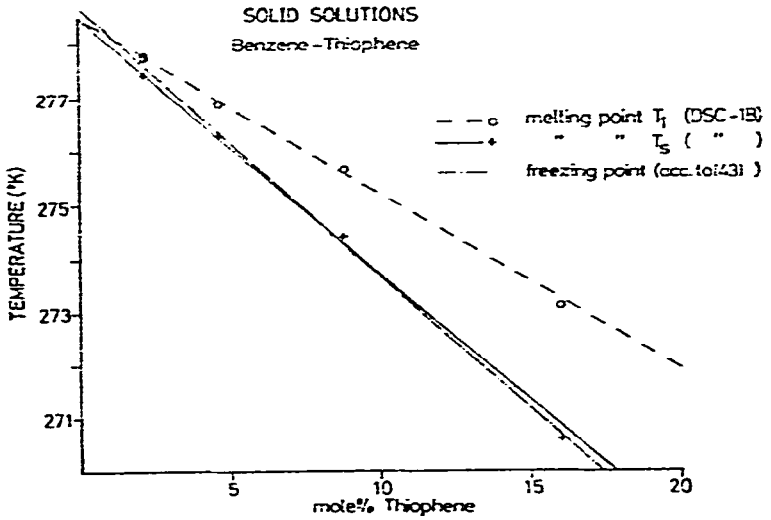

Fig. 9. Solid solutions of benzene–thiophene. Presentation of melting point *vs.* concentration of thiophene in the measured systems.

The heat of fusion is, in contrast to eutectic systems, practically constant with increasing amounts of impurity. As reported at the Perkin–Elmer meeting in Zurich[42], in 1969, we obtained similar values for the impurity and heat of fusion for the same system as reported by Driscoll *et al.*[6]. With careful calibration of the temperature scale of the DSC-IB, we were able to get absolute values of the melting points within ± 0.3 °C of the benzene–thiophene samples. In Fig. 9 the melting points of the samples calculated with a computer program based on Eqn. (7) are presented as a function of the thiophene concentration. The melting points of the samples, T_s, agree with literature values found from freezing point measurements by Fawcett and Rasmussen[43]. The decrease of the melting point of the pure component, T_1, is incompatible with the assumption of a eutectic system.

The decrease of T_1 with an increasing concentration of thiophene is explained by the phase diagram of a complete series of solid solutions of benzene–thiophene.

From our measurements, we conclude that a temperature accuracy of the DSC-IB in the order of $\pm 0.3\,^{\circ}C$ enables the detection of at least 1 mole-% of thiophene. In order to measure the amount of impurity forming solid solutions in a binary system, one has to determine, with test measurements on the same binary system, the shift of the melting point as a function of the concentration of the impurity. For binary and multicomponent systems with unknown impurities, a significant change of the melting point T_i indicates one or several possible effects, *e.g.* solid solutions, polymorphism, salt or solvate formation of the main component, decomposition, etc.

In conclusion, we can state that in a great number of pseudobinary systems, it is possible to measure impurities forming solid solutions with the main component but with the restriction that the impurities are known. At present, one is not able to measure absolute amounts of impurities in systems of solid solutions with unknown components.

THE PRACTICAL ASPECTS OF DSC PURITY MEASUREMENTS

(*a*) *Experimental technique*

The experimental procedure for a purity determination with the DSC apparatus, in the case of a substance investigated for the first time, is as follows.

DSC curves of the substance under investigation are recorded from room temperature, or from at least 30 °C below the melting region up to 100 °C above the melting point in the case of low-melting substances. The curves are measured with a high scan speed (*e.g.* $dT/dt = 16\,^{\circ}C\ min^{-1}$) in the volatile as well as in the open sample pan. This procedure enables energy changes to be observed in addition to the heat of fusion, caused by effects such as; modification changes, eutectic points, evaporation of impurities, loss of crystal water, and decompositions. The measured DSC curves enable us to form the substances into three groups: (*1*) Substances with no effect observed other than the melting in the given temperature region; (*2*) substances with effects clearly separated from the melting region; and (*3*) substances with effects interfering with the melting region.

This discussion is restricted to substances without effects interfering with the melting region; such an effect is one that occurs within the linearization region used in the computing procedure of the purity value. The investigation of effects other than the melting observed with the DSC apparatus is an analytical problem involving thermogravimetrical analysis, X-ray and spectroscopical methods and other appropriate methods.

The same samples used for the first DSC curves are cooled down for recrystallization and heated up again to get a second melting curve, if possible. The second melting curve yields information about a modification change which could occur during the recrystallization, about the stability of the substance in the temperature region scanned, and about effects which can be observed by a comparison of the curves from the first and second melts.

If a second melting curve cannot be obtained because the substance has

decomposed during melting or did not recrystallize, the stability is determined by keeping a sample at constant temperature for 3–30 minutes at about 10 °C below the melting point. Such a procedure, with respect to the thermal treatment, is not completely equivalent to a second melting.

If such a thermal treatment indicates a decomposition of the substance, the samples are enclosed in volatile sample pans inside a glove box filled with nitrogen gas. The measurements in a nitrogen atmosphere reveal the answer to the question of the oxygen sensitivity of the substance under investigation.

Finally, some melting curves are selected for an evaluation with the computer. The results of the computer program are listed and then compared with the corresponding melting curve and with the information available from other analytical methods. After following this procedure there is a strong basis for setting up an instruction for routine work on the same substance.

Routine analyses are normally performed with one or two melting curves under appropriate conditions. In the case of routine substances without any anomaly, the evaluation of the melting curve is performed according to the method suggested by Plato and Glasgow[31] or with a computer program.

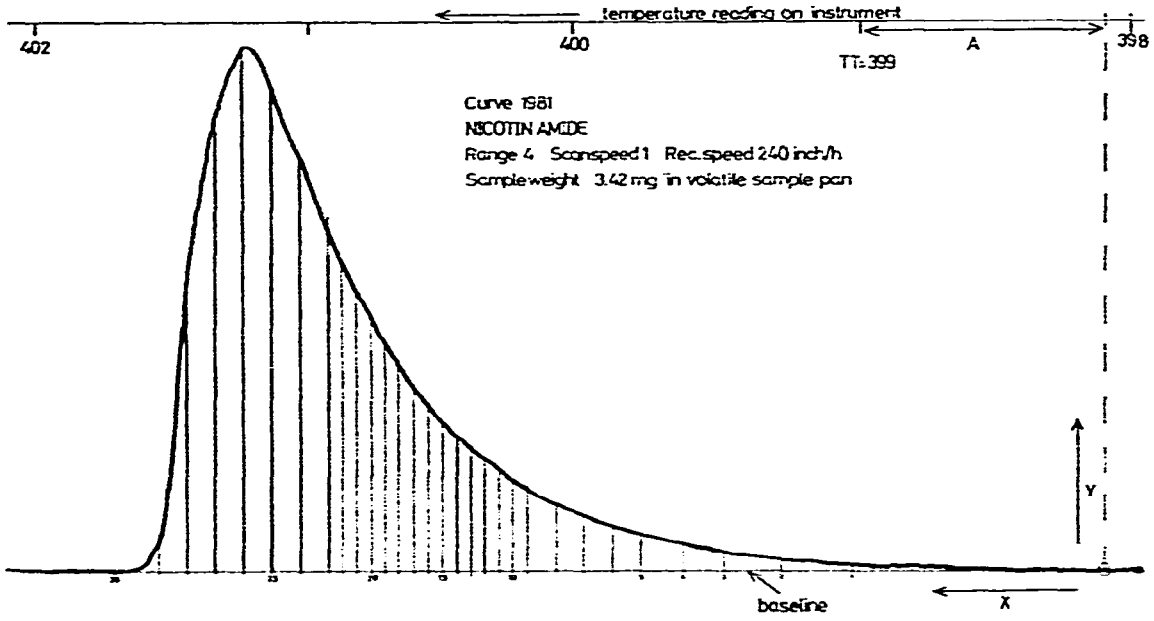

Fig. 10. DSC melting curve of nicotinamide (number of curve 2, 1981).

(b) The evaluation of melting curves in this laboratory

The evaluation of melting curves and the basic computer program for the purity determination will be discussed in some detail because of the importance of the evaluation with respect to the whole issue of the purity determination by DSC. The evaluation of melting curves will be discussed with nicotinamide as an example. A

typical melting curve of a sample of nicotinamide measured with the DSC-IB is shown in Fig. 10. The conditions for this melting curve are: sample weight, 3.42 mg; range, 4 mcal sec^{-1}; scan speed, 1 °C min^{-1}; and recorder speed, 240 in. h^{-1}.

The evaluation of the melting curve starts with the drawing of a baseline, as shown in Fig. 10. The baseline connects the pretransition to the posttransition region with a straight line. The points 0–30 are marked on the baseline, observing the rule that the density of the points should be greater in the expected linearization region than in the other parts of the melting curve. The temperature TT (399 °K in the case of nicotinamide) and the distance A are necessary for the connection of the points on the x-axis (see Fig. 10) to the temperature marking of the instrument. The point number zero is the zero point for both the x- and y-ordinates. The values (x_i, y_i) for the points $i = 0$–30 are used as a representation of the melting curve in the computer program. The main program calls up the subroutines. Each of the subroutines can be briefly described as follows:

Subroutine INPUT: Reads and writes experimental data.

Subroutine DATEN: Contains the calibration factors of the instrument and calculates the constants for the temperature correction.

Subroutine INTGR: Performs the integration of the melting curves and corrects the temperature for all experimental points.

Subroutine SUBXQ: Calculates the molten fraction r using the values obtained from subroutine INTGR.

The molten fraction r_i is given by

$$r_i = \frac{\sum_{n=1}^{i} a_n}{\sum_{n=1}^{30} a_n} = \frac{a_{0,i}}{a_{0,30}} \tag{40}$$

where a_n is the area bounded by the baseline, the melting curve and the lines perpendicular to the baseline through the points i and $i-1$ ($i = 1$–30). The baseline is shifted with the parameter ax set to zero at the beginning of the linearization and set to 10 cm^2 for the first linearization step. The molten fraction r_i' is calculated according to the equation

$$r_i' = \frac{a_{0,i} + ax}{a_{0,30} + ax} \tag{41}$$

The variation of the parameter ax within the linearization procedure is performed in subroutine VORFIT.

Subroutine VORFIT: This subroutine tests the curvature of the transformed melting curve in the $(1/r, T)$-diagram inside the given linearization region (for a molten fraction of about 10–40%). The curvature is determined with segments between transformed points i and $i+j$, with i and $i+j$ restricted inside the linearization region, and for $j = 2, 3, 4, 5, 6$, etc.

When the curvature of the transformed melting curve is convex downwards, the distance between the curve and segments (calculated only for the transformed experimental points) is positive according to our definition, and is counted as an element of class *N1*. When the curvature is convex upwards, all the points are counted as class *N2*. The predominant curvature inside the linearization region is proportional to the absolute value of $\Delta N = N1 - N2$ and the sign of ΔN indicates whether the curvature is convex upwards or downwards. The sign of the parameter ax for the first linearization step is the same as the sign of ΔN calculated at the beginning of the linearization. Again, the values of *N1*, *N2* and ΔN are determined with the shifted values of the molten fraction according to Eqn. (41). If the sign of ΔN is not changing, the parameter $2ax$ is used for the second linearization step. If the sign of ΔN changes in the second linearization step, the parameter $0.5ax$ is applied to the next linearization. The linearization with the diminution of the parameter ax is performed until one of the following conditions is reached: (*i*) $|N1 - N2| \leqslant 1$; (*ii*) $|ax_{old} - ax_{new}| \leqslant 0.5\ \mathrm{cm}^2$; or (*iii*) the number of steps is greater than 50.

The value of the parameter ax for the last linearization step is called POPTA, given in the printout as the value relative to the total area of the melting curve $a_{0,30}$

$$\mathrm{POPT} = \frac{\mathrm{POPTA}}{a_{0,30}} \times 100 \tag{42}$$

With a parameter value of $ax = 10\ \mathrm{cm}^2$ at the beginning of the linearization, condition (ii) can be fulfilled within 5 linearization steps.

Subroutine FIT: The linearization in this subroutine starts with the last parameter value POPTA taken from the subroutine VORFIT. The subroutine performs a least-square fit with the parameter values POPTA, POPTA$\pm AX$. The parameter value AX is set to $0.5\ \mathrm{cm}^2$ at the beginning. The sum of the squares of the deviation of the transformed points with respect to the regression line is minimised by changing the parameter AX. The least-square fit terminates under any of the following conditions: (*i*) $AX \leqslant 10^{-2}\ \mathrm{cm}^2$; (*ii*) when the number of steps is greater than 30; or (*iii*) when the sum of the squares of the deviation of the transformed points from the regression lines is $\leqslant 10^{-5}$.

Subroutine KONZ: The subroutine KONZ calculates with the aid of Eqn. (7) the information which one can get from the regression line and the conditions of the last linearization step.

Subroutine CHECK: The subroutine CHECK calculates the distance between the transformed points and the regression line. The greatest distance within the linearization region is called DTMAX. The distance of transformed points outside the linearization region is compared with DTMAX. Any point with a distance less than DTMAX is added to the linearization region. The first point, beginning with the linearization limits, with a distance greater than DTMAX interrupts the enlargement of the region in this specific direction. If the distances of the points adjacent to the limits of linearization are greater than DTMAX, the enlargement of the linearization region is attempted by multiplying DTMAX by a factor f. The values of the factor f

```
2  1981          NICOTINSAEUREAMID
-------------------------------------------------------------

EINWAAGE              =     3.4200  (IN MGR)                    TG-ALPHA  =     3.1200
MOLEKUL ARGEWICHT     =   122.1300  (IN GR)                     ALPHA     =    -0.1030
RANGE                 =     4.0000  (IN MCAL/SEC)             BETA      =    41.2900  (IN GRAD)
RANGE-FAKTOR          =     0.9640  (IN MCAL/(CM**2))          A         =     8.9000  (IN CM)
SCAN SPEED            =     1.0000  (IN GRAD/MIN)             B         =     9.8000  (IN CM)
                                                              TT        =   399.0000  (IN GRAD KELVIN)
                                                              ZVOR      =   240.0000  (IN INCH/H)
DTMAX                 = 0.4888E-02  GRAD                      NPOT      =     1       (1=FLUESSIGKEITS-,2=NORMALREHAELTER)


RESULTATE DES FIT-PROGRAMMS (MIT   0*DTMAX):

GRENZEN  J1 =  10 ;   J2 =  22                                SCHMELZBEREICH B(J1) =  12.18 %   B(J2) =  38.04 %
POPT                  =     2.06 %                            VON FN(J0)           =   160.74           CM**2
SCHMELZTEMPERATUR  (T0) =  127.27   GRAD CELSIUS               DELTA-H=F            =  5647.40           CAL/MOL
SCHMELZTEMPERATUR  (TS) =  127.22   GRAD CELSIUS               KONZENTRATION DER VERUNREINIGUNG =    0.0953 +- 0.0029MOL-%
STEIGUNG DER GERADEN (S) =   -0.054 +-  0.0016                KRYOSKOPISCHE KONSTANTE          =   -0.57           GRAD/MOL-%
Q.-SUMME DER Y-ABWEICHUNGEN: M-1/R GROSS =  0.1214E-03        M-1/R KLEIN =  0.4099E-04
 * * * * * * * * * * * * * * * * * * * * * * * * * * * * * * * * * * * * * * * * * * * * * * * * * * * * * * * * * * * *


RESULTATE DES FIT-PROGRAMMS (MIT   1*DTMAX):

GRENZEN  J1 =  10 ;   J2 =  26                                SCHMELZBEREICH B(J1) =  10.34 %   B(J2) =  73.43 %
POPT                  =    -0.03 %                            VON FN(J0)           =   160.74           CM**2
SCHMELZTEMPERATUR  (T0) =  127.24   GRAD CELSIUS               DELTA-H=F            =  5531.76           CAL/MOL
SCHMELZTEMPERATUR  (TS) =  127.20   GRAD CELSIUS               KONZENTRATION DER VERUNREINIGUNG =    0.0737 +- 0.0081MOL-%
STEIGUNG DER GERADEN (S) =   -0.0427 +-  0.0047               KRYOSKOPISCHE KONSTANTE          =   -0.58           GRAD/MOL-%
Q.-SUMME DER Y-ABWEICHUNGEN: M-1/R GROSS =  0.2955E-03        M-1/R KLEIN =  0.9659E-03
 * * * * * * * * * * * * * * * * * * * * * * * * * * * * * * * * * * * * * * * * * * * * * * * * * * * * * * * * * * * *


RESULTATE DES FIT-PROGRAMMS (MIT   5*DTMAX):

GRENZEN  J1 =   9 ;   J2 =  26                                SCHMELZBEREICH B(J1) =  10.04 %   B(J2) =  73.69 %
POPT                  =     0.82 %                            VON FN(J0)           =   160.74           CM**2
SCHMELZTEMPERATUR  (T0) =  127.24   GRAD CELSIUS               DELTA-H=F            =  5578.55           CAL/MOL
SCHMELZTEMPERATUR  (TS) =  127.20   GRAD CELSIUS               KONZENTRATION DER VERUNREINIGUNG =    0.0788 +- 0.0087MOL-%
STEIGUNG DER GERADEN (S) =   -0.0453 +-  0.0050               KRYOSKOPISCHE KONSTANTE          =   -0.57           GRAD/MOL-%
Q.-SUMME DER Y-ABWEICHUNGEN: M-1/R GROSS =  0.4241E-03        M-1/R KLEIN =  0.5955E-03
 * * * * * * * * * * * * * * * * * * * * * * * * * * * * * * * * * * * * * * * * * * * * * * * * * * * * * * * * * * * *


RESULTATE DES FIT-PROGRAMMS (MIT  10*DTMAX):

GRENZEN  J1 =   8 ;   J2 =  26                                SCHMELZBEREICH B(J1) =   9.16 %   B(J2) =  73.91 %
POPT                  =     1.83 %                            VON FN(J0)           =   160.74           CM**2
SCHMELZTEMPERATUR  (T0) =  127.25   GRAD CELSIUS               DELTA-H=F            =  5634.50           CAL/MOL
SCHMELZTEMPERATUR  (TS) =  127.20   GRAD CELSIUS               KONZENTRATION DER VERUNREINIGUNG =    0.0857 +- 0.0094MOL-%
STEIGUNG DER GERADEN (S) =   -0.0488 +-  0.0053               KRYOSKOPISCHE KONSTANTE          =   -0.57           GRAD/MOL-%
Q.-SUMME DER Y-ABWEICHUNGEN: M-1/R GROSS =  0.8071E-03        M-1/R KLEIN =  0.6623E-03
 * * * * * * * * * * * * * * * * * * * * * * * * * * * * * * * * * * * * * * * * * * * * * * * * * * * * * * * * * * * *
```

Fig. 11. Nicotinamide, printout for curve 2, 1981.

are specified in the program as $f = 5$, 10, 15, 20, etc. The linearization procedure (subroutine VORFIT, FIT and KONZ) is performed again in each linearization region, which is found by enlargement. In routine work the computer program is restricted to three enlargements of the linearization region.

In Fig. 11 the printout for nicotinamide is shown together with the experimental conditions and the calibration factors of the instrument. The distance DTMAX is calculated as 4.8×10^{-3} °C. The first linearization region covers the melting region from 12.18 to 38.04% or from point 10 to point 22. The parameter POPT is 2.06%, which means that the baseline is shifted slighiy downwards. The melting points are: $T_1 = 127.27$ °C and $T_s = 127.22$ °C. The melting points yield a slope of the regression line of -0.05 °C. The heat of fusion is 5650 cal mole^{-1}. The concentration of the impurity is 0.095 ± 0.003 mole-% and the cryoscopic constant according to Eqn. (2) is 0.57 °C mole-%$^{-1}$. The enlargement of the linearization region to a linearization region from 9.16 to 73.91% indicates only small variations in the melting points, heats of fusion and concentrations of impurity.

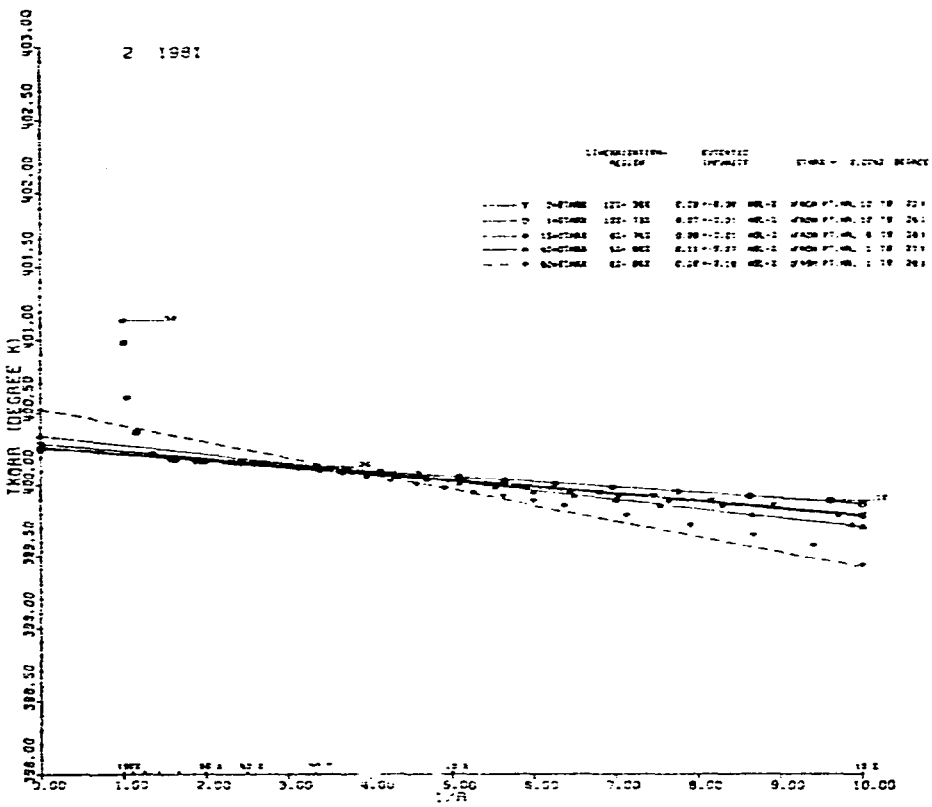

Fig. 12. (1/r, T)-diagram for nicotinamide.

The (1/r, T)-diagram of nicotinamide is presented in Fig. 12. The transformed points of the melting curve of nicotinamide are shown and also the regression lines

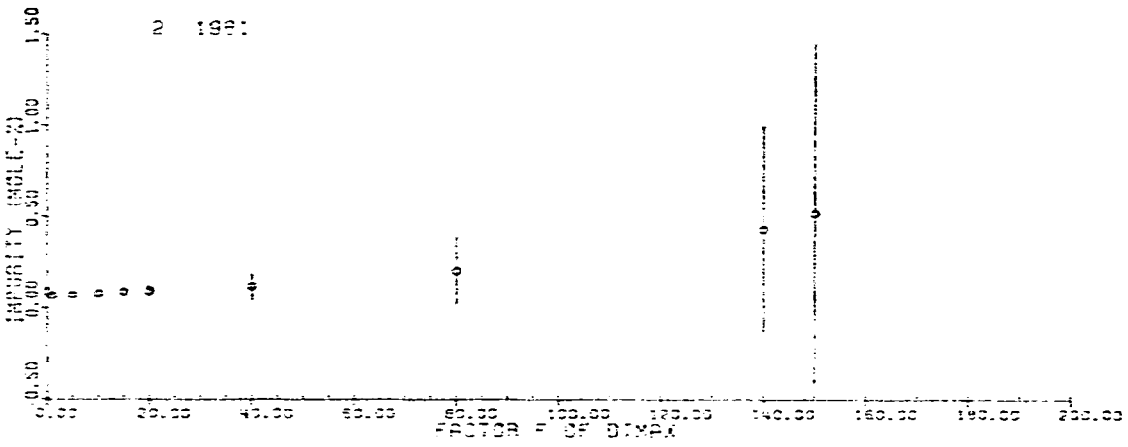

Fig. 13. Presentation of the impurity content of nicotinamide (number of curve 2, 1981) *vs.* the factor *f* of DTMAX.

calculated with points inside the linearization regions. In Fig. 13 the concentration of the impurity as a function of the distance *f* (DTMAX) is presented. The errors of the impurity concentration with 65% confidence limits, calculated with the regression line within the linearization region, are shown as lines through the corresponding points. The linearization region for the *f*-factor of 80 covers the molten fraction from 8 to 96% with a concentration of the impurity of nicotinamide of 0.20 ± 0.18 mole-%; a value which is consistent with the result from the first linearization region. The molten fraction from 8 to 96% covers a part of the melting curve from point 1 to point 28 (see Fig. 10). The point 26 is certainly an upper limit for the linearization region, which in the presented evaluation of the melting curve for nicotinamide implies an *f*-factor of 15 as an upper limit. The agreement between the results for these restricted linearization regions is even better.

The conclusion from such results on impurity values and thermodynamic constants, which are nearly independent of the melting region selected for the calculation, are a necessary but not sufficient condition for an ideal melting behaviour of a substance.

EXPERIMENTS AND DISCUSSION

(*a*) *High purity substances*

A few high purity substances are listed in Table XI. The melting curves of these substances were measured in volatile sample pans and the evaluation was performed according to the method explained in the preceding section, part (*b*). The cryoscopic constants of substances measured with the DSC-IB differ by less than 14% from literature values.

The difference is mainly caused by the heat of fusion measured with the DSC-IB. For high purity substances a 10% error in the evaluated heat of fusion will lead to only a negligible error in the eutectic impurity.

TABLE XI

PROPERTIES OF SOME HIGH PURITY SUBSTANCES

Substance	*Melting points (°K)*		*Difference in melting points* $\Delta T = T_1 - T_s$ (°C)	*Heat of fusion* $\Delta H_{f,1}$ (*cal mole*$^{-1}$)	*Cryoscopic constant* k_T (°C *mole-%*$^{-1}$)	*Eutectic impurity* (*mole-%*)
	T_1	T_s				
Deionized water						
DSC	273.261	273.230	0.031	1650	0.90	0.035
Lit.	273.16			1434	1.04	
Benzene (Merck)						
DSC	278.561	278.490	0.071	2180	0.71	0.10
Lit.	278.66			2350	0.67	
Anthraquinone						
DSC	557.9	557.7	0.043	8400	0.75	0.06
Lit.	558.6			7800	0.86	
Carbazole						
DSC	517.51	517.38	0.013	6500	0.82	0.15
Lit.	518.5			7040	0.86	
4-Acetaminophenol	441.67	441.62	0.051	7280	0.53	0.09
Nicotinamide	400.42	400.37	0.05	5650	0.57	0.09
Irgafen	481.117	481.110	0.007	7140	0.70	0.01
Development compounds						
MA 731, Batch 2	372.55	372,53	0.02	6710	0.33	0.06
MA 849, Batch 1	392.52	392.48	0.04	7770	0.40	0.10

(*b*) *Mixtures of standard substances*

Experiments with mixtures of standard substances are discussed. The mixtures were prepared in a laboratory type ball-mill grinder. In Table XII the actual and measured impurity values for the system phenacetin–*p*-aminobenzoic acid (*p*-ABA) are compared.

TABLE XII

COMPARISON OF THE ACTUAL AND MEASURED IMPURITY VALUES FOR THE PHENACETIN–*p*-AMINOBENZOIC ACID SYSTEM

Main component	*Scan speed* $\frac{dT}{dt}$ (°C *min*$^{-1}$)	*Added p-ABA* (*% by weight*)	*Actual impurity* $n_{v,a}$ (*mole-%*)	*Measured impurity* $n_{v,m}$ (*mole-%*)	$\frac{n_{v,a} - n_{v,m}}{n_{v,a}} \times 100$ (%)
Phenacetin	1	0.2	0.43	0.38	+12
	1	0.4	0.70	0.59	+16
	1	0.6	0.96	1.06	−10
	1	0.8	1.23	1.29	−5
	1	1.0	1.50	1.79	−19
	2	1.0	1.50	1.52	−1
	2	1.0	1.50	1.49	+1

The impurities were measured in normal sample pans and the evaluation was performed by the simplest method suggested by Perkin–Elmer[13]. The agreement between actual and measured impurity is reasonable.

Impurity with a high vapor pressure — In the next step, measurements in different sample pans were carried out in the melting region with an impurity of high vapor pressure. The system chosen was phenacetin–acetanilide (ACD), the results are presented in Table XIII. This system was chosen to emphasize the importance of the type of sample pan used for analytical purposes.

TABLE XIII

INFLUENCE OF AN OPEN AND CLOSED SAMPLE PAN ON THE MEASURED IMPURITY IN THE CASE OF AN IMPURITY WITH A HIGH VAPOR PRESSURE

Substance	*Sample pan*	*Number of melt*	*Actual impurity (mole-%)*	*Measured impurity (mole-%)*	*Weight loss of sample pan during melting* $\times 10^{-6}$ *g*
Phenacetin	normal	1		0.20	−7
OAS		2		0.36	−20
		3		0.29	−30
Phenacetin	volatile	1		0.46	−1
OAS		2		0.35	−1
		3		0.28	0
Phenacetin	normal	1	2.4	1.27	−15
OAS		2		1.11	−31
+1.6% (w/w) ACD		3		0.97	−46
		4		0.86	−62
Phenacetin	volatile	1	2.4	1.51	+1
OAS	sample pan	2		1.23	+2
+1.6% (w/w) ACD	without inside	3		1.36	+2
	cover	4		1.44	−2
Phenacetin	volatile	1	2.4	1.73	0
OAS	sample pan	2		1.27	0
+1.6% (w/w) ACD	with inside cover				

Compared with the sample weight of about 3 mg, a remarkable loss of weight from the normal pans is observed. The measurements of the weights of the pans were carried out with a Cahn Electrobalance before and after the melting of the samples. The measured impurity for the pure main component, phenacetin OAS, taken as a mean value of the three consecutive melts, is in the volatile sample pan only 0.1 mole-% higher than in the normal pan. With the absolute value of about 0.4 mole-% for the impurity measured in the volatile sample pan for phenacetin OAS, it was calculated as a rough approximation (setting mole-% equal to % by weight) that the total amount of impurities in a sample was about 12×10^{-6} g. The total amount of impurities is, as may be seen from Table XIII, about equal to the weight loss from a normal pan during each melting run. A loss from the sample pan of 4×10^{-6} g of impurity would have a remarkable influence on the melting curve. No shift of the

eutectic impurities to lower values with increasing number of melts was observed. The conclusion is that the vapor pressure of all the eutectic impurities of phenacetin OAS must be very small compared with the main component. This condition must be fulfilled over the whole temperature range in the region of melting.

The pseudobinary system of phenacetin OAS and acetanilide melted in the normal pan shows a measured value for the eutectic impurity of only 50% of the actual impurity for the first melt, and only 36% for the melt number 4. The total amount of ACD in a sample is 48×10^{-6} g. A loss of 50% of ACD as eutectic impurity during the first melt is equal to 24×10^{-6} g. This amount has to be compared with a total loss out of the sample pan of 15×10^{-6} g. The loss out of the sample pan consists mainly of ACD. Such a conclusion may be drawn from the vapor pressure data of phenacetin and ACD. The vapor pressure of phenacetin for 115°C is 3.2×10^{-2} torr according to the measurements of Wiedemann[38]. For ACD, Cramer[39] has reported a vapor pressure at 115°C of 6.3×10^{-1} torr. If we make the assumption that the loss out of the sample pan is only caused by ACD, we would have to explain the difference between the loss of ACD from the melt and the total loss from the sample pan. There are two possible explanations: (*1*) The heat of evaporation caused by the loss of ACD from the sample pan is superimposed upon the heat of fusion. (*2*) The ACD evaporates from the liquid phase onto positions inside the sample pan which have a lower temperature compared to the melt.

Explanation *1* can be excluded by a rough calculation of the heat necessary for the loss of about 24×10^{-6} g ACD measured from the first melt, when compared with the heat of fusion necessary for the melting of a 3 mg sample; in our example the heat of evaporation is about 2% of the heat of fusion. This energy of evaporation is further spread over the whole temperature region of the melting process. Therefore, the calculated eutectic impurity is influenced only to a rather small extent.

In contrast, point *2* is somewhat more reasonable, because of the great temperature gradient inside the sample pan, caused by the construction of the DSC-IB sample pan holder.

The transport of the ADC inside the sample pans is also indicated by the measurements in the volatile sample pans with and without an inside cover. However, the difference between the actual and the measured impurity is least in the volatile sample pan with an inside cover.

(*c*) *Different evaluation procedures applied to systems of phenacetin and benzamide*

In the next experiments, several evaluation procedures on systems of phenacetin and benzamide are discussed. Phenacetin was chosen as the main component and benzamide as the so-called impurity. The evaluation procedures of the melting curves are compared with the results of the actual and the measured impurity, with the melting points, and with the heats of fusion. The evaluation procedures applied to each of the melting curves are described briefly.

Evaluation procedure "Normal" (*N*) — This evaluation procedure is based on Eqn. (7) and is explained in detail in the preceding section, part (*b*).

Evaluation procedure "Square Root" (SR) — The evaluation procedure SR uses the following equation

$$T = \frac{T_1}{2} + \frac{T_1}{2}\left[1 + \frac{4RT_1}{\Delta H_{f,1}}\left(\ln\left(1 - \frac{1}{r}x_{0,2}\right)\right)\right]^{1/2} \tag{43}$$

Eqn. (43) is obtained from Eqn. (14) by the approximation $\Delta c_{0,i} = 0$. The evaluation procedure SR performs a trial and error method in varying the parameters T_1, $\Delta H_{f,1}$, and $x_{0,2}$.

With a set of parameters T_1, $\Delta H_{f,1}$, and $x_{0,2}$, together with chosen experimental values of the molten fraction r, values of T_C may be determined. These calculated temperature values, T_C, are compared with the experimentally obtained values of T, and the sum of the squares of deviation $T_C - T$ is computed for all experimental points within a given region of the molten fraction. With a three-parameter reiteration procedure, the sum of the squares of deviation is brought to a certain small limit, chosen from experience.

Evaluation procedure "heat of fusion" (HF) — The evaluation and linearization of the melting curve is performed with the evaluation procedure "Normal". The only deviation from the evaluation procedure "Normal" is within the subroutine KONZ. In the calculations of the eutectic impurity, using Eqn. (7), the heat of fusion of the main component is taken from the literature or from a measurement of a high-purity sample, whereas in the evaluation procedure "Normal", the heat of fusion used in Eqn. (7) is calculated from the melting curve of the sample under investigation.

Evaluation procedure "correction to the weight of the main component" (CMC) — The evaluation is performed with the procedure "Normal". In the subroutine KONZ we do not use the weight of the sample, but only the weight of the main component.

The results of the measurements on the phenacetin–benzamide system are presented in Table XIV.

In Table XIV are tabulated the concentration of the impurity; the actual impurity, which is known from the benzamide added plus the eutectic impurity of phenacetin OAS; the melting points; the heats of fusion; and the eutectic impurity calculated with the evaluation procedures described, N, SR, HF, and CMC. The measured eutectic impurity $x_{0,2}$ is a function of two parameters; the evaluation procedure and the concentration of the impurity itself.

The melting points will be discussed first. The melting points of the main component, T_1, are nearly constant up to a concentration of 10 mole-% of benzamide. For higher values of the impurity concentration, T_1 is about 3°C too low, but the correction of the thermal lag, caused by a scan speed of 16°C min^{-1}, is not easy. The melting point of the sample, T_s, decreases with increasing impurity content because of the melting point depression. The shift of T_1 for high impurity values, which was explained by experimental reasons, should have pratically the same influence on T_s. Therefore, the temperature difference $\Delta T = T_1 - T_s$, which is important for the

TABLE XIV

RESULTS OF SEVERAL EVALUATION PROCEDURES ON THE PHENACETIN OAS–BENZAMIDE SYSTEM

Main component, phenacetin OAS; impurity, benzamide.

Benzamide added (mole-%)	*Actual impurity (mole-%)*	T_1	T_s	*Evaluation procedure*							
				N		*SR*		*HF*		*CMC*	
				$\Delta H_{f,1}$	$x_{0,2}$	$\Delta H_{f,1}$	$x_{0,2}$	$\Delta H_{f,1}$	$x_{0,2}$	$\Delta H_{f,1}$	$x_{0,2}$
0		133.7	133.6	7860	0.22	7270	0.14	7750	0.21	7860	0.22
1.25	1.47	133.2	133.5	7330	1.39	7300	1.34	7750	1.47	7400	1.40
2.5	2.72	133.2	132.2	7040	2.0 ±0.4	7035	1.9 ±0.3	7750	2.2 ±0.3	7150	2.1 ±0.3
5.0	5.22	133.5	131.4	6960	4.5 ±1.0	7120	4.5 ±1.1	7750	4.9 ±0.8	7190	4.6 ±1.0
10.0	10.2	132.5	129.0	6535	6.9 ±1.0	6710	6.6 ±1.4	7750	8.2 ±0.6	7050	7.5 ±1.0
20.0	20.2	130.7	123.8	6100	13.0 ±1.4	6585	12.7 ±1.0	7750	16.5 ±1.3	7170	15.5 ±1.8
30.0	30.2	130.7	119.0	5896	21.2 ±1.8	6710	20.5 ±1.8	7750	27.8 ±1.9	7570	27.3 ±2.3

calculation of the impurity, should only be affected very slightly by the shift in T_1 and T_s.

The results of the eutectic impurities calculated according to the different evaluation procedures are practically constant for the high-purity substance phenacetin OAS (see Table XIV). The calculated eutectic impurities for systems with concentrations of 1.25, 2.5, and 5 mole-% of benzamide are all well within a normal error limit compared to the actual eutectic impurity (error limit up to ±10% relative to the impurity value).

The differences in eutectic impurities calculated with four different evaluation procedures in the concentration region of 10–30 mole-% of benzamide are remarkable. With the normal evaluation procedure N, also with the evaluation SR, the eutectic impurities are found to be about 30% too low compared with the actual eutectic impurities. In contrast, the evaluation procedures HF and CMC show relative differences of only 10–20% between measured and actual eutectic impurities. The conclusion is that the normal and the square root evaluation methods are only capable of yielding good results in an impurity region up to 5 mole-%. The differences between the two procedures (N, SR) are so small that we do not use the square root method, which requires a much longer computing time than the evaluation procedure "Normal". The heat of fusion method is as easy as the "Normal" evaluation but one needs a high-purity standard or a literature value of the heat of fusion of the main component. The procedure "correction to the weight of the main component" can only be performed with known values of the weight of the main component. The CMC method is of theoretical interest, and the application to systems with unknown impurities would only be a rough approximation.

(*d*) *Variation of scan speed and the use of two different data collection systems for melting curves*

Measurements were performed on two systems: (*1*) Diphenyl as a high-purity substance; and (*2*) phenacetin OAS and 2.5 mole-% of benzamide. Also two systems for the collection of data were used for the measurements: (*1*) ERA, Digital Data Acquisition system; (*2*) Mauerhofer system by Ciba–Geigy, Basel. The ERA system collects data in the premelting, melting and postmelting range on magnetic tape. The data collection rate for our measurements was chosen as 20 points sec^{-1}. The Mauerhofer system was built by Ciba–Geigy, Basel. Here the data are collected on paper tape. The data collection rate for this system is 2 points sec^{-1}.

The experimental data collected from melting curves with both of the systems replace the 31 experimental points (x_i, y_i) in the evaluation procedure "Normal". The baseline of the melting curves, which is drawn by hand in the procedure "Normal", is calculated, in the case of the data systems, from points in the premelting and the postmelting ranges. If the number of experimental points in the melting region is too high (ERA system), a reduction in the number of points is obtained by forming a mean value from 10 or 20 adjacent points. Such a data reduction has a smoothing effect on the experimental curve.

The eutectic impurities calculated from melting curves recorded either with the ERA or the Mauerhofer system are presented in Table XV. The experimentally varied parameter in the table is the scan speed.

TABLE XV

EUTECTIC IMPURITY AS A FUNCTION OF SCAN SPEED FROM MELTING CURVES RECORDED WITH THE TWO DIFFERENT DATA COLLECTION SYSTEMS

Scan speed (*°C min*$^{-1}$)	*Eutectic impurity (mole-%)*		
	ERA system	*Mauerhofer system*	*Mettler DTA-2000 and CT system*[c]
Diphenyl			
0.5	0.13	0.08	0.12
1	0.20	0.05	0.13
2	0.16	0.07	0.12
4	0.23	0.05	0.25
8	0.20	[a]	0.88
Phenacetin OAS–2.5 mole-% Benzamide[b]			
4	2.4	2.7	
8	2.2	2.2	
16	2.3	2.2	
32	2.6	[a]	

[a] No evaluation possible. [b] Actual eutectic impurity, 2.7 mole-%. [c] Values added in proof.

The melting of diphenyl is extremely sharp because of the purity level; on the other hand, the melting region of phenacetin–benzamide is rather broad. Equilibrium conditions between temperature and the molten fraction are calculated from Eqn. (7)

and used in the computing procedure. Non-equilibrium conditions, which would be expected at high scan speeds and for high-purity substances, should have an influence on the eutectic impurity calculated with Eqn. (7) with the aid of a linearization in the ($1/r$, T)-diagram. The variations of the calculated impurities with the scan speed for each of the substances within each of the data collection systems are rather small, and there is no significant shift of these eutectic impurities as a function of the applied scan speed.

For diphenyl, the mean value of the eutectic impurity for the scan speed in the range 0.5–8 °C min^{-1} is 0.18 ± 0.04 in using the ERA system for the data collection, and 0.06 ± 0.02 in the scan speed range 0.5–4 °C min^{-1} for the Mauerhofer data system. The difference is rather large, but one has to take into consideration that the melting curves were measured with two different DSC-IB instruments and two different data collection systems. In the case of the phenacetine–benzamide system, the agreement between the actual and the measured eutectic impurities is reasonable for all the scan speeds applied.

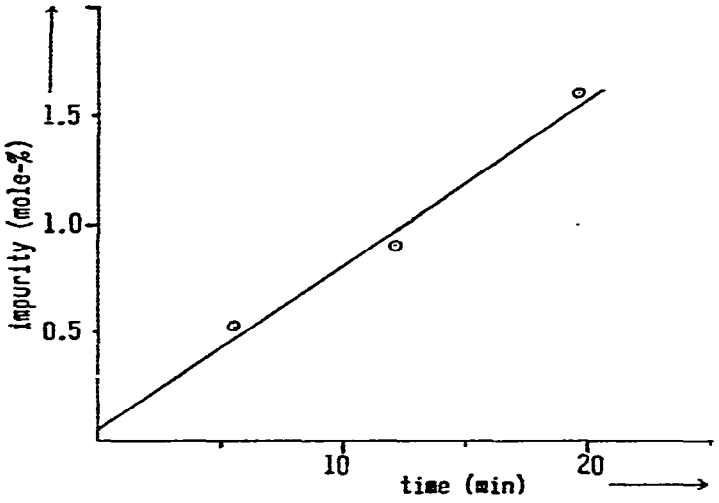

Fig. 14. Presentation of the decomposition of a sample of the development compound MA 1219 in a nitrogen atmosphere.

(*e*) *Purity measurements on substances which decompose in the melting region*

In the preceding section, part (*a*), we explained the necessary investigations on a substance which decomposes in the melting region. Melting curves are measured on the same substance with different thermal treatments. The calculated eutectic impurities of such melting curves are presented as a function of the time for which the substance was kept at a temperature close to the melting point with, of course, a correction for the time necessary for the melting. The measurements are performed in a nitrogen atmosphere in almost every case. An example is given in Fig. 14. The decomposition of this substance in a nitrogen atmosphere is calculated to be

TABLE XVI
COMPARAISON OF PURITY VALUES

Substance	*Batch No.*	*Sum of impurities*						
		Thermobalance (weight-%)	*DSC*		*TLC (%)*	*GLC (%)*	*Titration (%)*	*NMR*
			Volatile sample pan (mole-%)	*Open pan (mole-%)*				
Chlorpromazine-HCl	1	0.40	2.7	1.0	1.0	2.0		
Chlorpromazine-HCl	2	0.40	2.8	1.7	1.8	2.6		
Diazepam (1. Provenance)			0.4		0.10–0.15			
Diazepam (2. Provenance)			4.0		4.5–5.0	4.4		
Ethacrynic acid	1	0.05	1.6		1.1			
Ethacrynic acid	2	0.15	2.4	2.3	0.2			
Tolbutamide	1		1.8		1.6			
Cyclohexenylamine-HCl	1		0.6		pure	0.1		
Cyclohexenylamine-HCl	2		0.7		pure	0.1		
4-Acetaminophenol	1		0.09		0.1			
Nicotinamide	1		0.09		pure	0.02		
MA 731	1		0.9		0.6			
MA 731	2		0.4		0.2			
MA 956	1		0.2		0.05			
MA 956	2		0.1		0.05			
MA 1219	1		1.6		0.2			0.5 H_2O
MA 587	1	1.2	0.8		2–5		1.8–2.3	
MA 1017	2		1.0		pure			
MA 1017	2		1.0		pure	1.05		
MA 1017	4		1.5		0.15	1.2		
MA 1017	5		0.6		0.2	0.07		
MA 1469	3		0.2		0.02	pure		
MA 1769	3		0.4		pure	0.04		

0.075 mole-% min^{-1}. The eutectic impurity of the substance without thermal treatment (extrapolation of the thermal treatment to zero time) is 0.1 ± 0.1 mole-%. With air as the atmosphere for the melting, we observed a similar decomposition of the substance. This example shows the possibility of measuring impurity values of substances which are unstable in the melting region.

COMPARISON OF PURITY INFORMATION ON SEVERAL SUBSTANCES ACCORDING TO DSC, THERMOBALANCE, TLC, GLC, NMR-SPECTROSCOPY AND TITRATION

In Table XVI, a comparison of impurity values on substances obtained from several analytical methods is presented. The values headed "thermobalance" in Table XVI give the loss of weight of the substance up to the melting point. With a high amount of impurities of high vapor pressure in the melting region, one may expect quite a difference in the DSC values measured in the volatile and the open sample pan, as is seen for chlorpromazine–HCl. For many substances shown in Table XVI we see quite a reasonable agreement between the DSC values of impurities compared with the values from other analytical methods. However, there are substances like MA 1219 with a remarkable difference between the given impurity values. Such differences in impurity values obtained by several analytical methods provide a wide spectrum of problems to be solved with the appropriate investigations.

SUMMARY

The identification of substances and the determination of the purity of organic and inorganic substances by measurement of the melting point dates back to the early days of chemistry. In the 1920's Johnston and Giauque[3] introduced another thermal method for the purity determination of substances: the method of premelting. The method of Johnston and Giauque is based on a measurement of the heat of premelting of a substance as a function of temperature. The calorimeters used for the determination of the heat of premelting were built for sample weights up to several hundred grams. Relaxation times for the thermal equilibrium and the equilibrium of mass in the order of hours resulted from the large mass and the geometry of the calorimeters used in these investigations. In the 1960's a calorimeter (DSC) was developed by the Perkin–Elmer Corporation, which allowed the measurement of heats of premelting of a substance for samples of a few milligrams. The relaxation time for the DSC is in the order of parts of a second. The new instrument brought a fast development and a broad application of the method of premelting especially for purity measurements of pharmaceutical and agrochemical substances. Perkin–Elmer improved the DSC with the development of two further instruments: the DSC-IB and the DSC-2. All these three instruments are constructed according to the same basic principle, *i.e.* the measurement of temperature and heat of premelting, but differ in features such as: calorimetric sensitivity, baseline stability, temperature range, temperature calibration linearity and performance of the temperature programmer. Other instruments like

the DTA 2000 from Mettler Corporation, the Du Pont 900 can also be used for purity determinations.

In the literature mainly results on high purity substances are reported. A limitation of the purity region from 95 or even from 99 to 100% is claimed. These limitations of the method are substantiated by several authors because of marked differences between the actual and measured purity values. The discrepancies are explained in literature in terms of an inconsistency between the simplest equation for the solubility equilibrium and the melting behaviour of organic substances. We found that this explanation appears to be only one of several possibilities; other reasons may be the following: anomalous behaviour of main component and impurities, experimental conditions, recording system and data collection, and evaluation procedure—including the chosen equation for the description of the solid–liquid equilibrium—applied to the measured melting curve.

An investigation of these alternative reasons are rather cumbersome in the case of multi-component systems because of the multiplicity of the physical and chemical properties of all the components. Furthermore, the following aspects affecting the purity values should be considered: (i) the measurement of melting curves in open and closed sample pans, (ii) the use of different scan speeds, (iii) the measurement of a first and a second melting curve of the same sample, (iv) the influence of oxygen on the chemical stability of a substance in the melting region, (v) the proof of the ideality of a melting curve, and (vi) the evaluation of melting curves with a high enough number of data points and with the appropriate evaluation procedure.

It may be concluded from statements in the literature on the accuracy of purity values that there are two regions of purity with an arbitrary separation limit of 99 mole-%. The probability of a good agreement of actual and measured purity values is high in the high-purity region, and low in the low-purity region.

The work in our laboratory was concerned with a thorough investigation of effects causing these inconsistencies. Binary eutectic mixtures were selected as test systems, because phase diagrams, physical and chemical properties are easily found in literature. Using different equations for the description of the solubility equilibrium we have calculated theoretical phase diagrams and theoretical melting curves. The comparison of theoretical and experimental phase diagrams gives a measure of the quality of the approximation attained by the chosen equation for the solubility equilibrium. The study should be extended to include the influence of the activity coefficient on theoretical phase diagrams. Theoretical melting curves are useful for a proof of the ideality of experimental curves which is important for the reliability of calculated purity values.

Another application of theoretical melting curves is the determination of purity values by comparison of the experimental curves with a set of theoretical curves. These are calculated by selecting an equation for the solubility equilibrium, and transforming it into a function describing the theoretical melting curve (a so-called specific heat function). Thermal constants of the corresponding main component and a purity value are then inserted into the equation of the specific heat function.

Calculation and presentation of the specific heat functions for a set of purity values can be executed by computer. The comparison of the experimental curve with specific heat functions is performed either visually or by a least-square fit.

The transformation of theoretical melting curves calculated from the simplest equation of the solubility equilibrium on a temperature scale, $T-\Delta T$, is also of theoretical importance. The temperature difference $\Delta T = T_i - T_1$ is given by the difference of the melting point of the corresponding main component T_i and an arbitrarily chosen reference temperature T_1. The ratio of a transformed theoretical melting curve and a reference melting curve with the same concentration of eutectic impurities taken at corresponding temperatures is constant and equal to $[1+(\Delta T/T_1)]^{-2}$. The transformation reveals the fact, that melting curves of different main components with different melting points but equal concentrations of eutectic impurities are rather similar in their shape.

Systems with a complete series of solid solutions are treated at the present time by the measurement of melting or freezing points. A strong restriction in the quantitative determination of solid solutions is the necessity of knowing the melting point of the impurity forming solid solutions with the main component. Of course, it would be even better to know the phase diagram of the main component and the impurity. The accuracy of the purity measurements of solid solutions is related to the accuracy of the temperature measurement of the instrument. The determination of solid solutions is impossible in most of the systems with more than one impurity forming solid solutions.

In the evaluation procedure of melting curves for eutectic impurities one should consider the importance of the following: (i) the evaluation of melting curves measured with scan speeds up to 32°C min^{-1} is only possible in connection with a fast data collection system, (ii) the linearization with a least square fit is not without problems in case of practical melting curves, (iii) the first linearization should be performed in a linearization interval from about 15 to 35% of the substance melted and the interval should be extended for a succeeding linearization, and (iv) the evaluation procedures suggested by several authors (*e.g.* Scott and Gray[18]) are limited to a high purity region. Melting curves of substances with low purity must be treated by an evaluation procedure which corrects among others for the heat of fusion of the main component.

Ten thousand melting curves for more than 500 different compounds were measured and evaluated in our laboratories with three DSC-IB calorimeters since 1968. Several test systems were investigated for an evaluation of practical and theoretical aspects of the purity determination by DSC. Results from other analytical methods, especially for pharmaceutical and agrochemical substances, have been compared with results from the DSC method.

ACKNOWLEDGMENTS

The author wishes to express his thanks to the following persons for collaboration in experimental and theoretical work: O. Heiber, G. Tonn, W. Huber, A.

Geoffroy, B. Humpert and U. Rudolf. The author is also grateful for many helpful discussions with: S. G. Lawrence, J. Meier, H. C. Mez, P. Moser, G. Rihs, K. Wunder and R. Zbinden.

REFERENCES

1 L. Kofler and A. Kofler, *Thermomikromethoden zur Kennzeichnung organischer Stoffe und Stoffgemische*, Verlag Chemie, Weinheim (1954).
2 A. Eucken and E. Karwat, *Z. Phys. Chem.*, 112 (1924) 467.
3 H. L. Johnston and W. F. Giauque, *J. Amer. Chem. Soc.*, 51 (1929) 3194.
4 G. Pilcher, *Anal. Chim. Acta*, 17 (1957) 144.
5 A. R. Glasgow, N. C. Krouskop, J. Beadle, G. D. Axilrod, and F. D. Rossini, *Anal. Chem.*, 20 (1948) 410.
6 G. L. Driscoll, L. N. Duling, and F. Magnotta, *Proc. ACSS on Analytical Calorimetry, San Francisco*, 1968, p. 271.
7 E. F. Joy, J. D. Bonn, and A. J. Barnard Jr., *Thermochim. Acta*, 2 (1971) 57.
8 S. V. R. Mastrangelo and R. W. Dornte, *J. Amer. Chem. Soc.*, 77 (1955) 6200.
9 B. Wunderlich and St. M. Wolpert, *Therm. Anal., Proc. Int. Conf., 3rd, Davos*, 1 (1971) 17.
10 G. J. Davis and R. S. Porter, *J. Therm. Anal.*, 1 (1969) 449.
11 N. J. De Angelis and G. J. Papariello, *J. Pharm. Sci.*, 57 (1968) 1868.
12 R. Schumacher and B. Felder, *Z. Anal. Chem.*, 254 (1971) 265.
13 *Thermal Analysis Newsletter, Nos. 5 and 6*, Analytical Division, Perkin–Elmer Corp., Norwalk, Conn., U. S. A.
14 E. M. Barrall II and R. D. Diller, *Thermochim. Acta*, 1 (1970) 509.
15 R. Reubke and A. Mollica Jr., *J. Pharm. Sci.*, 56 (1967) 822.
16 R. N. Rogers and E. D. Morris Jr., *Anal. Chem.*, 38 (1966) 410.
17 M. J. O'Neill, *Anal. Chem.*, 36 (1964) 1238.
18 L. A. Scott and A. P. Gray, *DSC-Purity and the DSC-4 Computer Program for Purity Analysis*, Norwalk, Conn., U. S. A., 1969.
19 H. M. Heuvel and K. C. J. B. Lind, *Anal. Chem.*, 42 (1970) 1044.
20 W. L. Gent, *J. Sci. Instrum.*, 2 (1969) 69.
21 K. S. Pitzer and D. W. Scott, *J. Amer. Chem. Soc.*, 63 (1941) 2419.
22 D'Ans-Lax, *Taschenbuch für Chemiker und Physiker*, 2 (1964) 1076.
23 *Ibid.*, 2 (1964) 1076.
24 *Ibid.*, 2 (1964) 1075.
25 *Ibid.*, 2 (1964) 1085.
26 *Ibid.*, 1 (1964) 380.
27 *Ibid.*, 1 (1964) 350.
28 W. Perron, *Therm. Anal., Proc. Int. Conf., 3rd, Davos*, 1 (1971) 35.
29 M. J. O'Neill and A. P. Gray, *ibid.*, 1 (1971) 279.
30 A. P. Gray, *Proc. ACSS on Analytical Calorimetry, San Francisco*, 1968, p. 209.
31 C. Plato and A. R. Glasgow Jr., *Anal. Chem.*, 42 (1969) 330.
32 E. Marti, O. Heiber, W. Huber, and G. Tonn, *Therm. Anal., Proc. Int. Conf., 3rd, Davos*, 3 (1971) 83.
33 F. D. Rossini, *Chemical Thermodynamics*, Wiley, New York, (1950) 298.
34 J. H. Hildebrand and R. L. Scott, *The Solubility of Nonelectrolytes*, Dover, New York, (1964) 13.
35 *Beilsteins Handbuch der Organischen Chemie*, 13 (1930) 461.
36 *Ibid.*, 9E1 (1932) 96.
37 H. Staude, *Physikalisch-Chemisches Taschenbuch*, 2 (1949) 1179.
38 H. G. Wiedemann, *Thermochim. Acta*, 3 (1972) 355.
39 J. S. N. Cramer, *Rec. Trav. Chim. Pays-Bas*, 62 (1943) 606.
40 L. Kofler, *Z. Anal. Chem.*, 128 (1948) 533.
41 R. Haase and H. Schönert, *Solid–Liquid Equilibrium*, Pergamon Press, Glasgow, (1969) 60.
42 E. Marti and O. Heiber, *Meet. on the Purity Determination with the DSC-1B*, Perkin–Elmer Corp., Zürich, 1969.
43 F. S. Fawcett and H. E. Rasmussen, *J. Amer. Chem. Soc.*, 67 (1945) 1705.